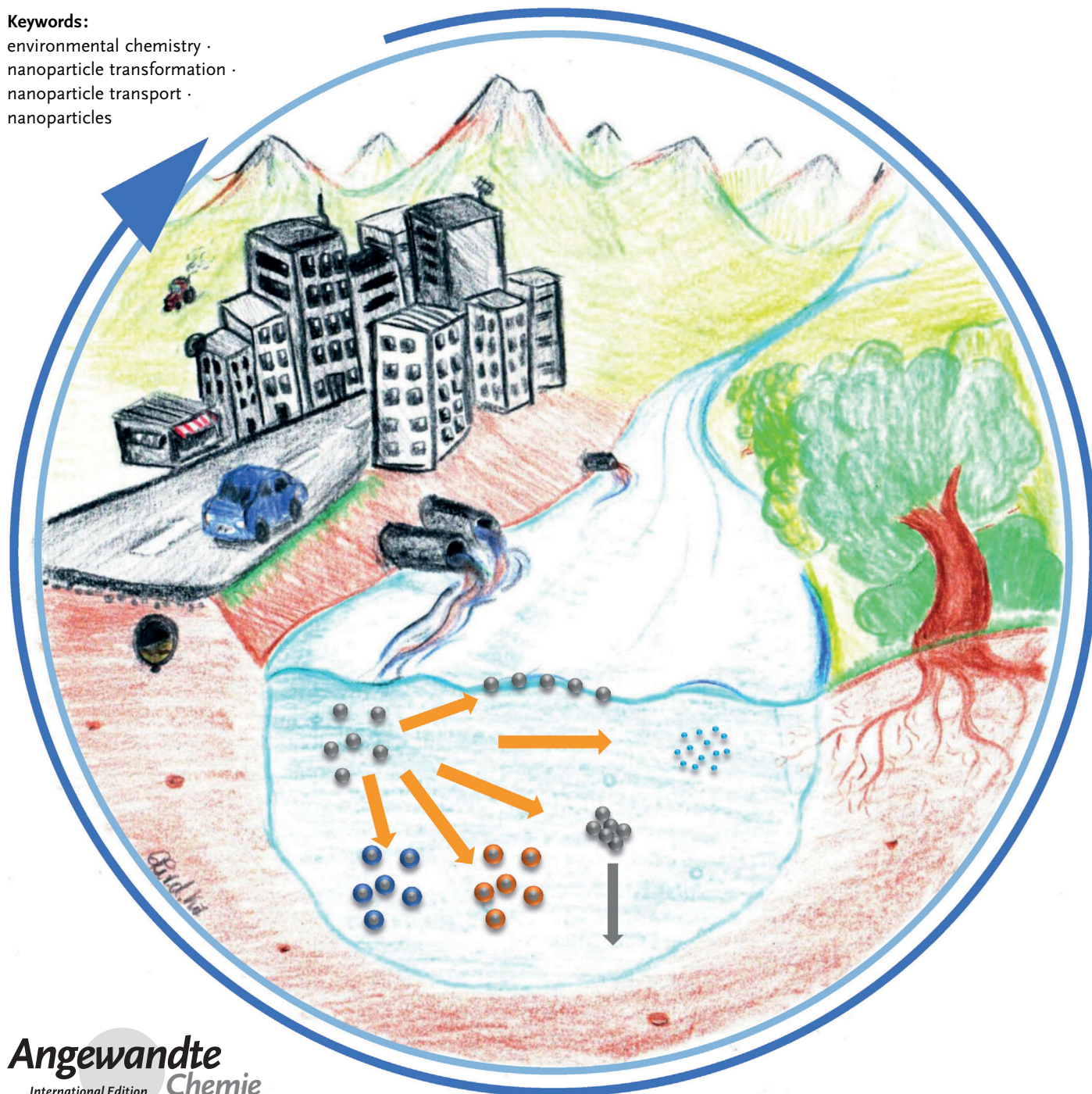


# Spot the Difference: Engineered and Natural Nanoparticles in the Environment—Release, Behavior, and Fate

Stephan Wagner, Andreas Gondikas, Elisabeth Neubauer, Thilo Hofmann, and Frank von der Kammer\*

**Keywords:**

environmental chemistry ·  
nanoparticle transformation ·  
nanoparticle transport ·  
nanoparticles



*The production and use of nanoparticles leads to the emission of manufactured or engineered nanoparticles into the environment. Those particles undergo many possible reactions and interactions in the environment they are exposed to. These reactions and the resulting behavior and fate of nanoparticles in the environment have been studied for decades through naturally occurring nanoparticulate (1–100 nm) and colloidal (1–1000 nm) substances. The knowledge gained from these investigations is nowhere near sufficiently complete to create a detailed model of the behavior and fate of engineered nanoparticles in the environment, but is a valuable starting point for the risk assessment of these novel materials. It is the aim of this Review to critically compare naturally observed processes with those found for engineered systems to identify the “nanospecific” properties of manufactured particles and describe critical knowledge gaps relevant for the risk assessment of manufactured nanomaterials in the environment.*

## 1. Introduction

The behavior and fate of naturally occurring nanoparticles (1–100 nm) and colloids (1–1000 nm) has been intensively studied for decades. However, the knowledge gained from these investigations is nowhere complete enough to create a detailed model of nanoparticulate behavior and their fate in the environment. It is known that processes such as surface reactions, stability, mobility, and dissolution play a major role in controlling their fate and behavior in the aqueous environment (Figure 1). The extent of these processes is regulated, among other things, by surface properties of the particles and environmental conditions such as pH value, ionic strength, and natural organic matter. Nowadays, the release of engineered nanomaterials (ENMs) as a consequence of increased production, use in consumer products, and industrial applications provokes questions regarding appropriate risk assessment strategies for the prediction of their fate and behavior in various environment media. The pivotal question, whether existing knowledge can be applied to predict the fate and behavior of ENMs, or if ENMs exhibit a distinct fate from natural nanoparticles, can be addressed by identifying the controlling processes of their fate and behavior in the environment. It is the aim of this Review to critically compare processes of naturally occurring nanoparticles with those observed for ENMs to identify the “nanospecific” properties of the latter and describe critical knowledge gaps relevant for their risk assessment in the environment. Furthermore, a decision tree model is presented, which enables us to decide what ENM-specific tests are required to determine the nanospecific properties.

The processes which affect the fate and behavior of nano iron oxide particles (NIOPs) are illustrated in Figure 1. NIOPs can dissolve or grow, can aggregate or be deposited on surfaces, can be coated with organic and inorganic constituents of water and/or can be transformed in terms of their crystal structure. The fate and behavior of the iron

## From the Contents

<b>1. Introduction</b>	12399
<b>2. Release</b>	12400
<b>3. Surface Modifications</b>	12403
<b>4. Particle Stability and Mobility</b>	12406
<b>5. Dissolution</b>	12412
<b>6. Summary and Conclusions</b>	12414
<b>7. List of abbreviations</b>	12416

particles is controlled by the hydrochemical conditions and the properties of the NIOPs. For example, the transport of natural NIOPs is regulated by

the  $\text{Ca}^{2+}$  concentration.<sup>[\*]</sup> Engineered NIOPs have a distinct shape, which is very homogeneous between particles compared to naturally occurring NIOPs (Figure 2). The question of whether this specific particle shape may control the fate and behavior of the engineered NIOPs is addressed in this Review.

The Review is based on a literature search, which followed the workflow depicted in Figure 3a. Literature was collected from a Scopus search (search criteria: keyword: engineered nanomaterials; environment, publication date after 2010). Additionally, a list of the most prominent authors in the field of the fate and behavior of engineered nanomaterials and natural colloids in the environment was compiled. Publications from these authors were added to the collection if missed by the keyword search. Collected publications were screened for relevant references, including publications before 2010. The selection process of publications and the subsequent topic-related categorization into subgroups was subdivided in three steps: I) A total number of 376 publications were evaluated according to the predefined quality criteria, which are listed in Figure 3a. II) All publications, which fulfilled the quality criteria were assigned to one of the main categories of natural colloids or engineered nanomaterials (Figure 3b). III) Both groups were further classified to one or more of the four subcategories (release, stability/transport, surface modification, and dissolution). The

[\*] S. Wagner, A. Gondikas, E. Neubauer, T. Hofmann, F. von der Kammer  
Department of Environmental Geosciences  
University of Vienna  
Althansstrasse 14, UZA II, Vienna, 1090 (Austria)  
E-mail: frank.von.der.kammer@univie.ac.at

© 2014 The Authors. Published by Wiley-VCH Verlag GmbH & Co. KGaA. This is an open access article under the terms of the Creative Commons Attribution Non-Commercial NoDerivs License, which permits use and distribution in any medium, provided the original work is properly cited, the use is non-commercial and no modifications or adaptations are made.

temporal development of the number of publications in the subcategories is depicted in Figure 3c.

## 2. Release

The overall environmental concern that may result from the use of nanotechnology in consumer and industrial products is a function of both the potential hazards related to the nanomaterials and the environmental exposure, that is, the concentrations at which these materials will be present in the environment. Besides newly developed specific nanomaterials, a number of materials which contain a nanoparticulate size fraction have been produced for a long time. A typical example is pyrogenic silica (SiO<sub>2</sub>), which has been

commercially available since 1942 (Aerosil). Without knowledge of the specific environmental behavior of a given particle type, an equal distribution in the aquatic environment must be assumed, which completely neglects the potential of elevated exposure at places where those particles accumulate predominantly (sinks). Although much research has focused on the hazard aspect of nano risk assessment, little is known about the potential exposure, that is, the current and future concentrations of ENMs in the environment and the heterogeneity of the distribution.<sup>[4]</sup> These concentrations are proportional to the amounts of ENMs released either intentionally or unintentionally from human activities (Table 1). Even though the importance of quantifying release levels is globally acknowledged, there are few data available because of issues related to market practices and technical obstacles. Information about how ENMs are distributed within consumer product categories is scarce; release coefficients during use, recycling, and disposal of products are unknown, while most release sources are nonpoint sources, for example, humans, households, etc.<sup>[5]</sup> The lack of data is substituted by modeling studies that utilize a fair amount of assumption- or probability-based approaches.<sup>[6]</sup> Comprehensive models are vital for estimating release levels; however, it must be noted that their validation is hampered by the current lack of techniques that are able to measure ENMs in real-world systems and distinguish them from a plethora of naturally occurring nanomaterials.<sup>[7]</sup> Furthermore, test procedures that are tailored for dissolved constituents are not likely to succeed for nanomaterials.<sup>[8]</sup>



*Stephan Wagner received his MSc from Dresden University of Technology and in 2005 joined a research company concerned with the treatment of mining-affected water bodies. He was involved in consulting on groundwater remediation as well as research in domestic and industrial wastewater treatment. In 2011 he completed his PhD at the Brandenburg University of Technology, Cottbus with Prof. Busch. Since 2012 he has been a postdoctoral researcher at the Department of Environmental Geosciences at the University of Vienna, focusing on the development of analytical methods for nanomaterials in consumer products.*



*Dr. Frank von der Kammer completed his PhD in 2005 at Hamburg University of Technology, in the Department of Environmental Science and Technology with Prof. U. Förstner. He is currently senior scientist and vice Head of the Department for Environmental Geosciences at the University of Vienna. Previously, he was a visiting professor at the Universities of Pau and Aix-Marseille, France. His research interests include environmental colloids, their dynamic behavior and interaction with trace elements, natural nanoscale processes, nanoparticle characterization, and engineered nanoparticles in the environment.*



*Andreas Gondikas studied Chemical Engineering at the National Technical University of Athens (Greece). After an MSc in Engineering Management and one year consulting at a company in North Carolina (USA), he moved to Duke University. He completed his PhD with Prof. Heileen Hsu-Kim in 2012 and then joined the group of Prof. Thilo Hofmann in Vienna, Austria, as a postdoctoral researcher, working with Dr. Frank von der Kammer on methods for detecting nanomaterials in the environment. His research interests include applications of nanomaterials in consumer products, their fate, and effect in the environment.*



*Elisabeth Neubauer studied Engineering Geology at the Graz University of Technology (Austria), followed by one year of consulting on hydrogeology, geothermics, and environmental issues. In 2009, she started her PhD with Prof. Thilo Hofmann and Dr. Frank von der Kammer at the University of Vienna. After graduation, she stayed as a postdoctoral researcher and worked on the quantification of metal oxide nanoparticles (TiO<sub>2</sub> and CeO<sub>2</sub>) in surface waters. In 2014, she joined Prof. Peggy O'Day at the University of California, Merced, where she studies the oxidative dissolution of biogenic uraninite in the presence of nitrate and iron.*



*Prof. Thilo Hofmann completed his PhD at the University of Bremen with Prof. H. D. Schulz in 1999 and his habilitation in 2002 at the Institute of Applied Geology at the Johannes Gutenberg-University Mainz, after two visiting professorships at the National University of Hoh Chi Minh City (2001) and Stanford University, Department for Civil Engineering (2002). He is the chair of Environmental Geosciences at the University of Vienna. Since 2012 he has been Dean of the Faculty of Geosciences, Geography, and Astronomy at the University of Vienna. He is vice president of the Water Chemical Society (GDCH) and the Austrian Society for Remediation Management.*

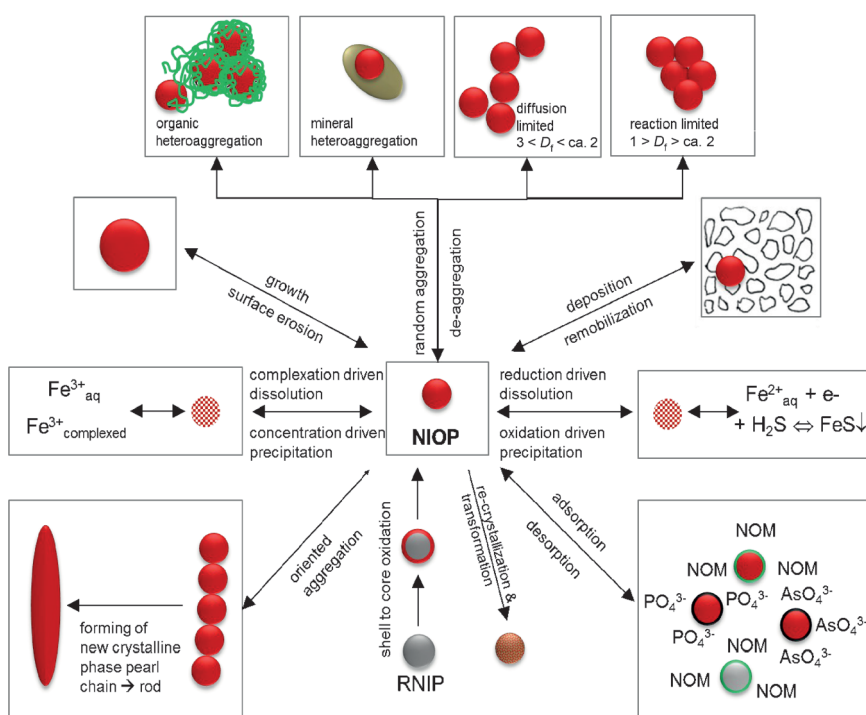


**Figure 1.** Graphical representation of possible reactions of nanoparticulate materials in natural aquatic media, with a nano iron oxide particle (NIOP) used as an example.

materials found in such locations.<sup>[12]</sup> Variations in the operation procedures at such facilities further complicate modeling efforts.<sup>[13]</sup> However, most challenging of all is determination of the accidental release at nonpoint sources, such as normal use and washing of ENM-containing sunscreen, cosmetics, and textiles.<sup>[14]</sup> The monitoring of such sources is restricted due to the large spatial and temporal variations in the use of ENM-containing products. However, as the need for environmental risk assessment increases, more detailed information is becoming available on global and regional levels, which will improve the material flow analysis of ENMs.<sup>[15]</sup> Besides production volumes, transfer factors of ENMs between the life-cycle stages are input parameters for such calculations. Examples of production volumes of ENMs are given in Refs. [12c, 15, 16], and [17]. SiO<sub>2</sub>, TiO<sub>2</sub>, and iron oxide (FeOx) belong to the group with highest production volumes and the predicted environmental con-

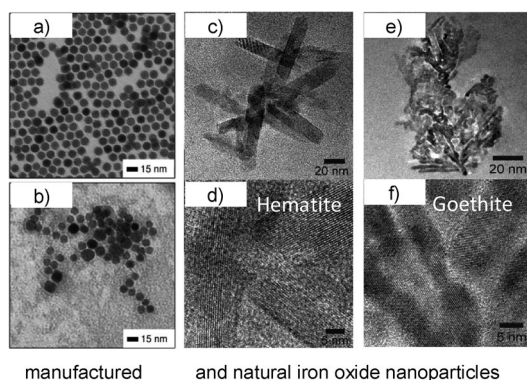


**Figure 2.** Electron micrographs of manufactured iron oxide nanoparticles applicable as contrast agents in magnetic resonance imaging (a, b, adapted from Hofmann et al.<sup>[2]</sup>) and natural iron oxide particles extracted from a floodplain sediment (c–f, adapted from Plathe et al.<sup>[3]</sup>).

Modeling the environmental concentrations of ENMs requires taking into account all the possible sources of ENMs released in the environment. This release can be intentional, for example, for remediation,<sup>[9]</sup> agricultural,<sup>[10]</sup> or water purification purposes.<sup>[11]</sup> These sources can be directly incorporated in release models, because of the availability of information regarding the amounts and characteristics of the ENMs used. More challenging is the unintentional release at point sources, such as wastewater treatment plants, waste incineration plants, manufacturing facilities, and possibly, in the near future, hospitals or clinics, because of the lack of information regarding the source and concentration of nano-

**Table 1:** Production volumes, predicted environmental concentration (PEC), environmental concentration (EC).

NP	Production within EU <sup>[16]</sup> [t/a]	PEC in surface water (Q <sub>0.15</sub> ; Q <sub>0.85</sub> )	Measured EC
TiO <sub>2</sub>	550 (55–3000)	0.53 (0.4; 1.4) µg L <sup>-1</sup>	0.55–6.48 µg L <sup>-1</sup> [26][a]
ZnO	55 (5.5–28 000)	0.09 (0.05; 0.29) µg L <sup>-1</sup>	n.a. <sup>[b]</sup>
SiO <sub>2</sub>	5500 (55–50000)	n.a.	n.a.
FeOx	550 (30–5500)	n.a.	n.a.
CeOx	55 (0.55–2800)	5.1–54.2 ng L <sup>-1</sup> [27]	n.a.
CNTs	550 (180–550)	0.23 (0.17–0.35) ng L <sup>-1</sup>	n.a.
fullerenes	0.6 (0.6–5.5)	0.11 (0.07–0.28) ng L <sup>-1</sup>	n.a.
Ag	5.5 (0.6–55)	0.66 (0.51–0.94) ng L <sup>-1</sup>	n.a.
quantum dots	0.6 (0.6–5.5)	n.a.	n.a.

[a] < 0.45 µm filtered. [b] n.a. = not available.

centrations are in the µg L<sup>-1</sup> range (Table 1). Much less significant in terms of production quantity are quantum dots, fullerenes, and Ag NPs. Determining the release levels of ENMs into the environment is a complicated task that requires not only the development of realistic modeling approaches but also their validation by techniques that are able to measure ENMs in complex real-world matrixes. Release of nanomaterial has been verified from paints that incorporate ENMs, either intentionally (silver nanoparticles)

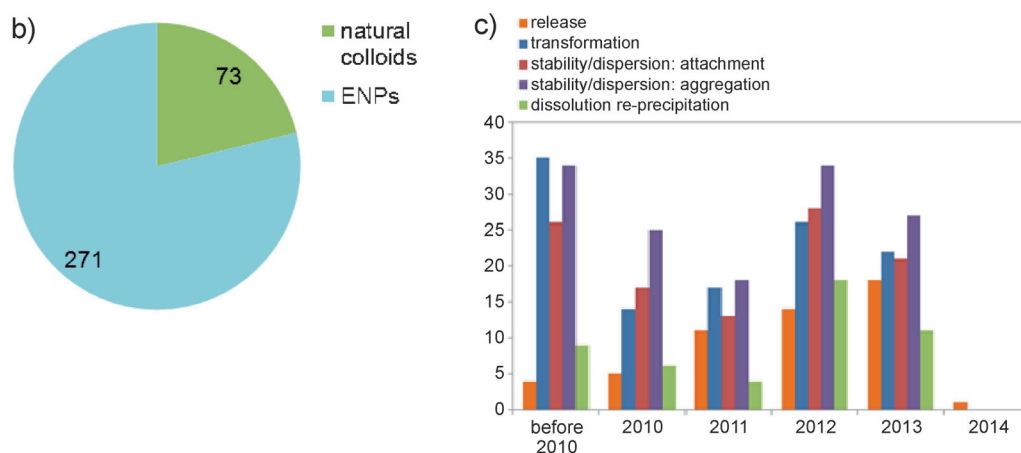
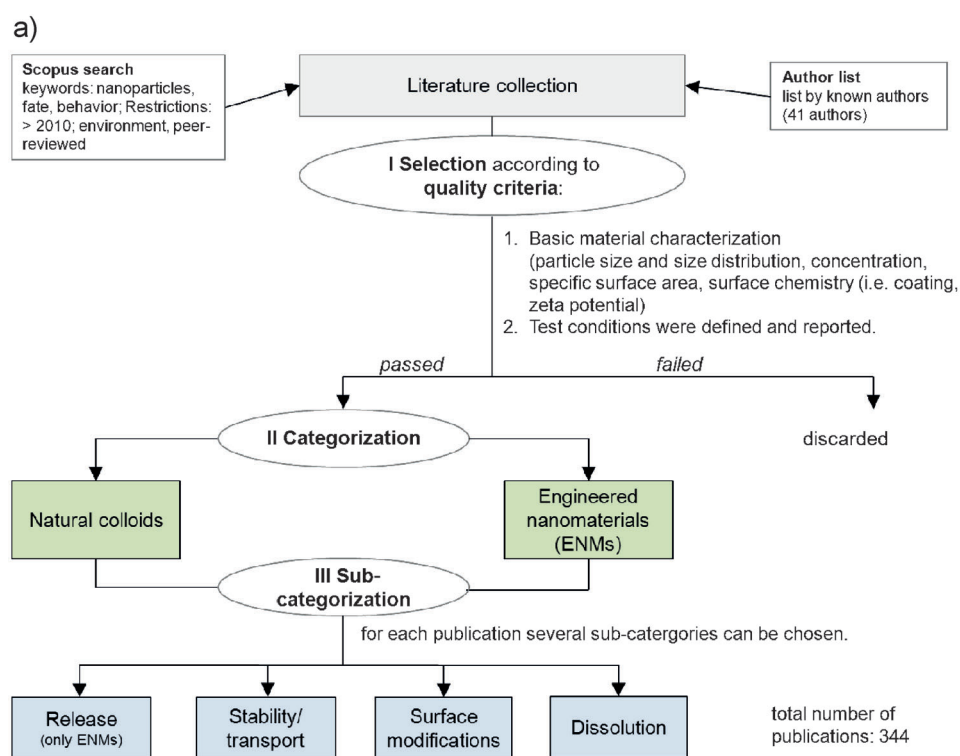


**Figure 3.** a) Selection and categorization scheme for evaluated publications, b) number of publications in the main categories, c) temporal development of the number of publications in the subcategories.

or unintentionally (titanium dioxide colloids with a fraction in the nano range).<sup>[18]</sup> Furthermore, there are a number of studies that report release data of ENMs during mechanical abrasion, for example, from a surface coated with ZnO or Fe<sub>2</sub>O<sub>3</sub>.<sup>[19]</sup> Particle release from a coated surface as a result of mechanical abrasion was found to be dependent on the type of coating and the surface. For example, mechanical abrasion by sanding of a polyurethane ZnO coating revealed maximum local particle concentrations between  $6.15 \times 10^2$  and  $6.36 \times 10^4 \text{ cm}^{-3}$  in the surrounding atmosphere, which was obtained under laboratory conditions. In practice, lower numbers would be expected because of particle aggregation and precipitation occurring in the sanding machine. However, the predicted concentrations are comparable with commonly

observed particle concentrations in street canyons ( $2.5 \times 10^4$ – $1.5 \times 10^5 \text{ cm}^{-3}$ ).<sup>[19a]</sup> The application of ENMs, mainly Ag ENMs, in textile industries derives from the antimicrobial properties of Ag ions. The release of Ag from textiles was studied, for example, by Benn and Westerhoff.<sup>[20]</sup> The release of Ag ENMs from consumer products and textiles was studied, for example, by Farkas et al., Kaegi et al., and Quadros et al.<sup>[14a,18a,21]</sup> The release of Ag from Ag-containing textile varied between 0.3 and  $377 \mu\text{g g}^{-1}$  textile during the first washing cycle and dropped significantly during subsequent washing cycles.<sup>[20,22]</sup> The migration of ENMs from solid polymers is of interest in the field of food packaging and has already been investigated for several ENMs, such as Ag, TiO<sub>2</sub>, and TiN.<sup>[23]</sup> The maximum release rates of Ag from food containers under acidic conditions is  $3 \text{ ng cm}^{-2} \text{ day}^{-1}$  at 20 °C.<sup>[24]</sup> These findings were confirmed by our own investigations. The rates of Ag ion release from an ENM-containing solid polymer were higher at elevated temperature (25 and 60 °C) and decreased as the particle size increased (project Nano-FCM, Austria, final report in preparation). A quantitative release of particles even after the application of mechanical stress was not observed. This contradicts literature data, where stress conditions such as thermal, mechanical (e.g. abrasion), or chemical stress caused a low level migration of the particles from a polymer into an overlaying liquid.<sup>[23,24]</sup> Carbon nanotubes (CNTs) are typically embedded in a solid matrix, such as composite polymer materials, and so their release is only expected during manufacturing, subsequent processing, and recycling.<sup>[25]</sup> Accordingly, their predicted environmental concentrations are in the  $\text{ng L}^{-1}$  range (Table 1). Materials such as quantum dots are mostly

incorporated in electronic products. Therefore, release scenarios into the environment do not exist.

All these studies tested samples in a relatively simple matrix, which were taken directly after the release and before they enter natural water bodies. The detection and characterization of nanoparticles in natural water has been achieved for natural nanoparticles (e.g. by Neubauer et al.)<sup>[28]</sup> and for ENMs in complex food matrices,<sup>[29]</sup> however the detection and characterization of ENMs in natural water samples is technically challenging because of the low concentrations and complex matrixes, combined with much greater levels of naturally occurring nanomaterials of often very similar composition. Recent studies have shown that the use of elemental ratios of bulk measurements is a promising tool for determining the amount of ENMs, as it takes advantage of the pristine nature of ENMs compared to their natural counterparts.<sup>[30]</sup>

Considering the inaccuracy of the calculated environmental concentrations, which is caused by the large variation in the release data, risk evaluations, which are commonly based on PEC/PNEC ratios (PEC = predicted environmental concentration; PNEC = predicted non-effect concentration), have to be interpreted carefully.<sup>[95]</sup> Additionally, risk evaluation has to consider that concentrations of the natural counterparts can be several orders of magnitude higher than the ENM concentration.<sup>[31]</sup> However, the risk of ENMs may originate from their distinct behavior compared to their natural counterparts, even if they are present in much lower concentrations. In the following sections, such differences will be elucidated by contrasting properties of natural colloids and ENMs. Subsequently, possible differences in the fate and behavior of ENMs and natural colloids will be identified.

### 3. Surface Modifications

The surface of nanoparticles and colloids is likely to undergo modifications in natural water sources through biotic and abiotic processes. Examples of such processes are the adsorption and desorption of organic and inorganic compounds, chemical reactions (e.g. reduction and oxidation), as well as recrystallization and oriented aggregation (Figure 4). All of these processes are dependent on the hydrochemistry of the waters and are strongly influenced by the presence of ligands, reducing or oxidizing agents, and the properties of natural organic matter (NOM).<sup>[14b]</sup> Surface properties are critical for the fate and bioavailability of particles in natural waters because they regulate particle interactions with colloids, surfaces, and biota (as investigated by e.g. Yoshida et al.).<sup>[32]</sup> Here, we summarize the current state of knowledge on the surface modification of ENMs, compare it with knowledge on naturally occurring colloids, and attempt to identify the processes that may produce modified ENMs that differ from modification products of their natural counterpart.

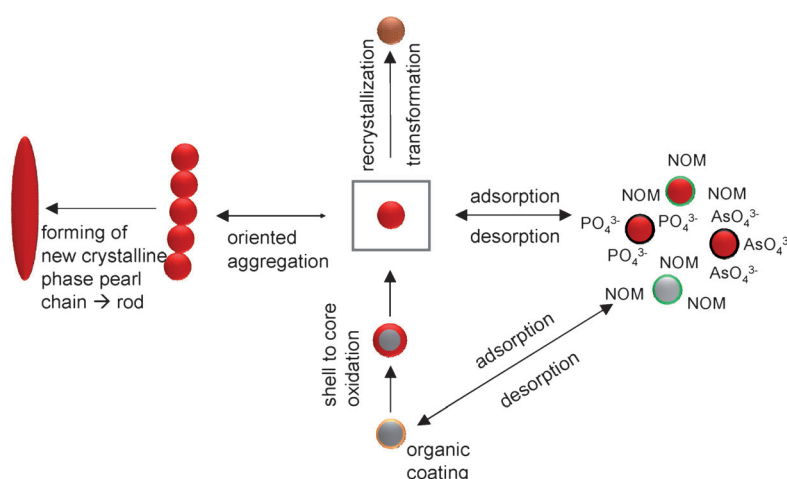


Figure 4. Main processes resulting in surface modifications of ENMs.

#### 3.1. Adsorption and Desorption

ENMs are often coated with engineered organic substances (often termed “organic coating”), whose role is to keep the particles evenly suspended in the product. This is achieved by inducing electric and/or steric repulsion between the particles or by increasing the viscosity of the media to minimize particle movement (e.g. in paints). These organic compounds are likely to be quickly desorbed or decomposed in natural aquatic systems. At the same time, because of their natural abundance in surface waters, NOM and inorganic ions are likely to adsorb on the surfaces of ENMs. The simultaneous desorption of nonpersistent engineered organic compounds and the adsorption of naturally occurring components strongly affects the fate and transport of ENMs by regulating the surface structure, charge, and charge homogeneity—properties that are critical for the dispersion, flocculation, and deposition of nanoparticles in the environment.

Several studies have dealt with the effect of the type of organic coating on the stability and reactivity of ENMs.<sup>[33]</sup> Low-molecular-weight organic coatings with charged functional groups induce electrostatic repulsive forces on particles, while long-chain polymers induce steric repulsion. The mode of attachment of the organic coating to the ENM surface, that is, inner- or outer-sphere complexes, the hydrophobicity, and the (bio)degradability of the organic coating are the most important properties that control the relative persistence of the organic coating on the ENMs. For example, polyethylene oxide is biodegradable<sup>[34]</sup> and polydimethylsiloxane (an organic coating that is used on titanium dioxide nanoparticles in cosmetic products) is readily removed from the surface of the particles in a simple water matrix.<sup>[35]</sup> However, organic ligands that form inner-sphere complexes with surface atoms of metal-containing nanoparticles are expected to be highly persistent.<sup>[36]</sup> TiO<sub>2</sub> ENMs used in sunscreen products contain two types of coatings: an inorganic layer, which is typically comprised of aluminum oxide or silica, to protect from surface reactions on the photochemically active TiO<sub>2</sub>, and an engineered organic coating to help keep the particles suspended in the product. The engineered

organic coating of the ENMs is readily removed in a simple water medium, but the inorganic coating is persistent.<sup>[35]</sup>

The extent of removal of the engineered coating from the surface of ENMs is partly dependent on the presence and properties of the NOM present. NOM is a large family of organic compounds that comprises a wide range of molecules and macromolecules, including humic and fulvic acids, extracellular polymeric substances, proteins, and low-molecular-weight organic compounds and ligands such as carboxy compounds, amines, and thiols. Therefore, it is very challenging to predict the interactions of NOM with particulate matter in natural aquatic systems. However, a lot of knowledge has been gained from research on simple aquatic systems. NOM may coat, stabilize, and therefore increase the mobility of virtually all ENMs. This is true for particles ranging from carbon-based particles, such as polystyrene NPs,<sup>[37]</sup> fullerenes, and carbon nanotubes,<sup>[37,38]</sup> to metallic and metal-based particles, such as Au,<sup>[37,39]</sup> Ag,<sup>[37,38b,40]</sup> TiO<sub>2</sub>,<sup>[41]</sup> and CeO<sub>2</sub> NPs.<sup>[42]</sup> Additionally, proteins and other macromolecules may stabilize a wide range of engineered nanoparticles (ENPs) in sludge,<sup>[37]</sup> and the interaction between proteins and NPs is influenced by the surface heterogeneities of the NPs, the size of the proteins, as well as the type of organic coating.<sup>[39,43]</sup> However, the formation of a protein corona on a nanoparticle is an unstable and reversible process when the protein and the NPs are of similar size.<sup>[42b]</sup> High concentrations of NOM may favor bridging coagulation.<sup>[41a]</sup>

The adsorption of NOM on NP surfaces is just as important for the colloidal stability of natural NPs as it is for ENMs. It can significantly affect their surface chemistry and resulting behavior in biological, technical, and environmental systems (see Ref. [44] and references therein). Organic compounds are able to stabilize a wide range of natural particles or particles that occur naturally in man-made systems, such as wastewater treatment plants, and enhance their transport in the environment. Several studies exist of the effect of NOM on the aggregation and attachment potential of metal-based nanoparticles, such as metal oxides (mostly iron oxides) and metal sulfides (e.g. CuS, ZnS, and HgS).<sup>[12a,28,45]</sup> The stabilization of NPs by NOM is an important mechanism for the mobility of metal or organic contaminants in surface or subsurface water.<sup>[1,3,46]</sup> NOM may also adsorb on top of organic coatings on ENMs and thus control the particles surface properties.<sup>[33c]</sup> The effect of NOM on the surface properties of ENMs depends on the type and properties of the organic coating and the NOM; for example, plant-derived NOM stabilized Ag NPs coated with polyvinylpyrrolidone (PVP) in a mesocosm study, but caused Ag NPs coated with gum arabic to be removed from the water column, likely by dissolution and binding of released Ag ions on sediment and plant surfaces.<sup>[40]</sup> PVP-coated Ag NPs have exhibited relative resistance against transformation across a wide variety of matrices, while NPs coated with gum arabic exhibit significantly higher transformation rates.<sup>[47]</sup> Ageing studies on Ag NPs in fresh water and marine environments showed that organic Ag such as thiol-bound Ag were the dominant species of Ag,<sup>[48]</sup> most likely as a result of the oxidation of Ag NPs by thiolate functional groups in the proteins or NOM.<sup>[49]</sup>

In addition to NOM, common inorganic groundwater constituents such as HCO<sub>3</sub><sup>-</sup>, HPO<sub>4</sub><sup>2-</sup>, SO<sub>4</sub><sup>2-</sup>, Cl<sup>-</sup>, and NO<sub>3</sub><sup>-</sup> may adsorb on the surface of particles and induce modifications that drastically alter the reactivity of the particle. For example, nanoscale zero-valent iron (nZVI) particles are prone to oxidation under typical environmental conditions, but the adsorption of NO<sub>3</sub><sup>-</sup> induces a passivating effect against oxidation.<sup>[50]</sup> Inorganic pollutants may sorb onto ENPs in aquatic and terrestrial environments.<sup>[51]</sup> For example, in soil mesocosms enriched with biosolids spiked with Ag NPs, TiO<sub>2</sub> NPs sorb Ag onto their surfaces.<sup>[51a]</sup> The interaction of ENPs with inorganic pollutants may lead to significant changes in the surface chemistry of the ENPs. One possibility is the formation of a surface layer with dimensions of several nanometers, which has been observed, for example, during fluoride uptake on hydroxyapatite.<sup>[51b]</sup> In addition to surface chemistry, inorganic ions affect the aggregation and deposition processes of NPs. The adsorption of multivalent inorganic cations, especially Ca and Mg, can suppress the stabilization effect of NOM (as seen, for example, by Kretzschmar et al.).<sup>[1]</sup> The aggregation rates of ZnO NPs are influenced by the adsorption of anions,<sup>[52]</sup> while the precipitation of inorganic pollutants such as Cr and As onto nZVI surfaces result in larger particle sizes and increased deposition of the nZVI.<sup>[51c]</sup> Finally, the presence of inorganic ligands may influence the crystal morphology and the growth kinetics during the oriented aggregation and transformation of ferrihydrite NPs into goethite.<sup>[53]</sup>

### 3.2. Chemical Reactions

Chemical reactions, for example, redox, precipitation, adsorption, complexation, and photochemical reactions take place on the surface of NPs when they are in contact with organic or inorganic ligands,<sup>[54]</sup> as well as main or trace water constituents.<sup>[52,53,55]</sup> These reactions can result in morphology changes, and likely formation of core-shell structures. NPs that are susceptible to redox reactions are metallic NPs, for example, Ag, Cu,<sup>[56]</sup> and nZVI,<sup>[50b,57]</sup> and metal oxide NPs, such as Fe oxides.<sup>[58]</sup> For example, nZVI corrosion has been reported in laboratory studies<sup>[50]</sup> and in the field.<sup>[59]</sup> Similar to natural NPs, reduction and oxidation reactions may occur when ENMs are transferred from oxic into anoxic environments or vice versa. The oxidation of Fe oxides such as magnetite may change the magnetic properties and, thus, the magnetic forces between particles, which influence the aggregation behavior of the material.<sup>[58a]</sup> Oxidation, therefore, could lead to decreased aggregation rates of magnetite NPs and a potential enhancement of their colloidal stability. In addition, the oxidation and reduction of Fe oxide NPs may have a large impact on the retention and release of sorbed contaminants such as arsenic.<sup>[58b]</sup>

The oxidation of surface atoms and the subsequent complexation with ligands is an important transformation process for metallic nanoparticles. In the case of Ag NPs, complexation with sulfides and chloride is likely. Complete or partial sulfidation was observed in Ag NPs that were dosed into sewage biosolids,<sup>[60]</sup> aerobic and anaerobic sludge,<sup>[61]</sup> in

raw wastewater,<sup>[62]</sup> (Figure 5), in a pilot wastewater plant,<sup>[63]</sup> and a simulated large-scale freshwater wetland with terrestrial soils and subaquatic sediments.<sup>[64]</sup> Nanosized AgS particles were also identified in the materials of the final-stage sewage sludge of a full-scale municipal wastewater

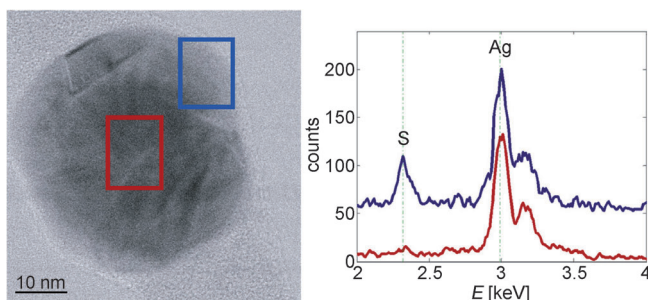


**Figure 5.** Left: Phase contrast bright field scanning transmission electron microscopy (STEM) image of an Ag NP collected from the sewer batch experiments (24 h). Right: EDX spectra revealing spatial variation in the S/Ag ratios (blue and red spectra).<sup>[62]</sup>

treatment plant.<sup>[65]</sup> The mechanism of sulfidation has been carefully studied. Liu et al. showed that the transformation at low sulfide concentration occurs through an oxidative dissolution/precipitation mechanism, which requires dissolved oxygen and with the creation of dissolved  $\text{Ag}^+$  as an intermediate; at high sulfide concentrations, the reaction occurred through direct particle–fluid reactions.<sup>[66]</sup>

The degree of sulfidation of Ag NPs depends on the available sulfide concentrations.<sup>[62,66,67]</sup> These results demonstrate that the surface of metallic nanoparticles is modified through redox reactions and the formation of a thermodynamically very stable complex. However, Ag originating from Ag NPs that had undergone partial or complete sulfidation remained bioavailable to plants and microbes,<sup>[60,64,67a]</sup> even though it has been shown that sulfidation may decrease the dissolution rate and thus the release of toxic  $\text{Ag}^+$  ions.<sup>[56b,67b]</sup> The release of  $\text{Ag}^+$  ions upon oxidative dissolution of Ag NPs can be systematically slowed by the binding of thiol and citrate ligands, formation of sulfidic coatings, or the scavenging of peroxy intermediates, and accelerated by preoxidation or reduction of the particle size.<sup>[56b]</sup> Chloride reacts with oxidized Ag NPs to form AgCl corrosion products.<sup>[68]</sup> Metallic Cu NPs oxidize quantitatively to  $\text{CuO}_2$  under low and neutral pH values and in the presence of citric and oxalic acid, while some of the CuO phase and even the Cu core may remain in pre-aged Cu NPs.<sup>[56a]</sup> These transformation reactions induce changes in the surface chemistry and heterogeneities of the surface charge, and thus affect, for example, the aggregation and sedimentation behavior of ENMs.

In addition to redox reactions, incident light can induce photochemical reactions of ENPs in surface environments. These may comprise the generation of free radicals, excitation of the photoactive material, and photodegradation. Carbon-based NPs such as carbon nanotubes and fullerenes are oxidized under UV irradiation.<sup>[69]</sup> Irradiation of ENPs enhances the production of reactive oxygen species, affects the

degradation of organic contaminants,<sup>[70]</sup> and may induce formation of aggregates,<sup>[69a]</sup> depending on the binding energy of the coating with the NPs. For example, Ag NPs coated with polyvinylpyrrolidone, which is believed to bind strongly to NPs, are stable under irradiation with sunlight. NPs coated with gum arabic, which binds more weakly to NPs, aggregate through strong oscillating dipole–dipole interactions.<sup>[71]</sup> Furthermore, the irradiation of NOM with sunlight can produce superoxide and hydrogen peroxide species that can reduce ionic silver to metallic silver nanoparticles,<sup>[72]</sup> or could potentially induce redox reactions on the particle surfaces, when NOM is sorbed on the particle. Metallic silver particles exhibited strong reactivity towards inorganic ligands, such as sulfide and chloride; the oxidation reactions require oxygen and result in complete oxidation of silver and the production of insoluble AgS and AgCl particles as well as dissolved silver chloride species.<sup>[66,73]</sup>

### 3.3. Oriented Aggregation

Nanoparticle growth through oriented aggregation has received a lot of attention in the past few years because of the unique nature of the aggregates. Oriented aggregation results in new NPs composed of crystallographically aligned primary particles.<sup>[74]</sup> A wide range of materials, including Fe oxides,<sup>[53,75]</sup>  $\text{TiO}_2$ ,<sup>[76]</sup> selenides, and sulfides may grow by oriented aggregation, and studies showed that this transformation process may also occur under environmentally relevant conditions. Oriented aggregation may involve phase transformation of thermodynamically less favorable minerals into more stable mineral phases, for example, the transformation of ferrihydrite into goethite,<sup>[75,77]</sup> with the rate of oriented aggregation depending on the size of the primary particles.<sup>[78]</sup> Such phenomena affect surface reactivity, and thus may have important roles in geochemical cycling. Oriented aggregation is a process that takes place in natural environments and is relevant for both natural and engineered nanomaterials. Burrows et al. studied the effect of ionic strength on the oriented aggregation of goethite nanorods from ellipsoidal ferrihydrite nanoparticles.<sup>[53]</sup> The size of the primary particle of the precursor was critical for the size and shape of the final product. Levard et al. observed that exposure of Ag ENMs to sulfide resulted in AgS being quickly formed on the surface of the particles.<sup>[67b]</sup> The resulting aggregated structures were mixed amorphous and crystalline AgS as well as the original form of metallic Ag, with the extent of sulfidation being dependent on the sulfide concentration. The final product particles were linked through AgS crystal bridges and demonstrated significantly less release of dissolved silver species compared to the original material.

### 3.4. Comparison of the Surface Transformations of Natural and Engineered Nanoparticles

Natural nanoparticles with similar compositions and transformation pathways as ENMs are present, and have

been present, in the environment for millions of years. Weber et al. demonstrated that natural NPs continuously undergo transformations when the biogeochemical conditions are changed in the pore water of a contaminated floodplain soil: Metallic Cu<sup>0</sup> colloids are formed through biomineralization. Sulfate reduction results in the transformation of the Cu<sup>0</sup> colloids into hollow copper-rich sulfide particles associated with bacteria, as well as into dispersed copper-rich sulfide NPs, which are probably formed through homogeneous precipitation.<sup>[46d]</sup> In addition, metallic silver nanoparticles are formed in natural conditions, under irradiation with sunlight, and metallic mercury may be formed under anoxic conditions by the reduction of Hg<sup>II</sup> from NOM.<sup>[79]</sup> The formation and transformation of sulfide colloids in the environment is strongly dependent on the biological activity.<sup>[80]</sup> For example, in sediment pore water, Hg<sup>II</sup> associates with sulfides and NOM to form chemical species that include organic-coated mercury sulfide NPs as reaction intermediates of heterogeneous mineral precipitation. Bacteria can methylate the mercury of HgS NPs and thus transform the mineral NPs.<sup>[80]</sup>

Studies on the reactions that may take place on the surface of ENMs go hand in hand with studies on the surface of naturally occurring particles. For example, zero-valent iron is oxidized in the environment to form iron minerals that are abundant in nature. NPs from Fe minerals are among the best studied natural NPs, and many transformation reactions have been documented. For example, schwertmannite (an iron oxyhydroxysulfate) recrystallizes into goethite (an iron oxide) when aged in water. However, adsorbed trace elements and organic macromolecules may suppress the transformation.<sup>[81]</sup> The oxidation of water that contains Fe-rich NPs may lead to extensive agglomeration of the Fe NPs and affect the interaction of Fe with NOM.<sup>[82]</sup> The adsorption of macromolecules on both natural and ENM surfaces can significantly affect their surface chemistry as well as their resulting behavior in biological and environmental systems (see Ref. [44] and references therein). This is, for example, important for the colloidal stability of natural NPs.<sup>[83]</sup> Interaction with common water constituents such as sulfide may decrease the surface charge of silver-, mercury-, copper-, and zinc-containing nanominerals and lead to aggregation.<sup>[45c]</sup>

It can be concluded that persistent organic coatings and core-shell structures differentiate ENMs from their natural counterparts through their surface transformations. Transformations of the NP coating modify the NP fate and behavior, since they control the NP flocculation and deposition. Another potential route to breaking down the coatings is biologically mediated transformation, for example, by biodegradation of polymer coatings covalently bound to nanomaterials.<sup>[34]</sup> Irrespective of the degradation mechanism, studies showed that the loss of the coating leads to aggregation of the particles.<sup>[35]</sup> Oriented aggregation results in new NPs composed of crystallographically aligned primary particles.<sup>[74]</sup> Evidence for oriented aggregation has been described for iron oxide coated sands,<sup>[84]</sup> and there are many examples where oriented aggregation plays an important role in, for example, biomineralization (see Ref. [74] and references therein).

## 4. Particle Stability and Mobility

Mobile natural colloids include silicates such as clay minerals, oxides and hydroxides of Fe and Al, colloidal silica, carbonates, organic matter, and “biocolloids” such as viruses and bacteria. These entities may interact with dissolved compounds, thus explaining the major importance of natural colloids for the transport of matter in aquatic environments. Such natural colloids can be mobilized (translocated), immobilized, or generated by changes in the geochemical and hydraulic parameters in aquifers or in surface waters (see Ref. [85] and references therein). The NP transport behavior in aquifers is governed by several processes (e.g. deposition, dissolution, filtration, aggregation; Figure 6). These processes are controlled by the properties of the NPs and the chemical conditions of their surroundings.

Numerous studies identified the surface-charge properties of colloids, in addition to their size and the Stokes settling velocity, as one of the quantitatively most relevant parameters for their transport behavior (e.g. the colloidal transport of natural clay and iron oxides studied by Kretzschmar et al.).<sup>[85,87]</sup> In surface waters, the surface charge of the particles determines the aggregation of the particles, which is one of the decisive processes for the stability of natural colloids (Figure 7). Unstable suspensions will aggregate, which leads to an increase in the particle size, and eventually to gravitational settling of the particles and a decrease in the particle number concentration. Particle transport in porous media is not only controlled by aggregation, additional processes such as particle deposition onto the porous media and size exclusion might affect the particle transport.<sup>[88]</sup> Particle transport in porous media is a function of particle surface charge, particle size, surface charge of the porous media, and spatial heterogeneity of the charge. These parameters are dependent on the composition of the particle and solid matrix as well as chemical and physical boundary conditions such as pH value, ionic strength (IS), and natural organic matter (NOM), which are termed key environmental factors. The significance of the listed key environmental factors for particle stability and mobility will be discussed in the following sections, followed by elucidation of the distinct behavior of ENPs.

### 4.1. Aggregation and Deposition

The extent of aggregation and deposition is determined by the surface chemistry of the particles and the porous media, as well as by the chemistry of the bulk solution.<sup>[89]</sup> If the aggregation occurs between similar surfaces, it is termed homoaggregation (Figure 7). In natural systems, there is a wide variety of different colloids with different surfaces and the environmental concentrations of natural counterparts are between one and seven orders of magnitude higher than ENPs.<sup>[31]</sup> Therefore, quantitatively more relevant is heteroaggregation, which is the aggregation of various particles such as environmental colloids.<sup>[90]</sup> The fundamental drivers of aggregation are Brownian motion, fluid motion, and differential settling. Brownian motion is the most significant

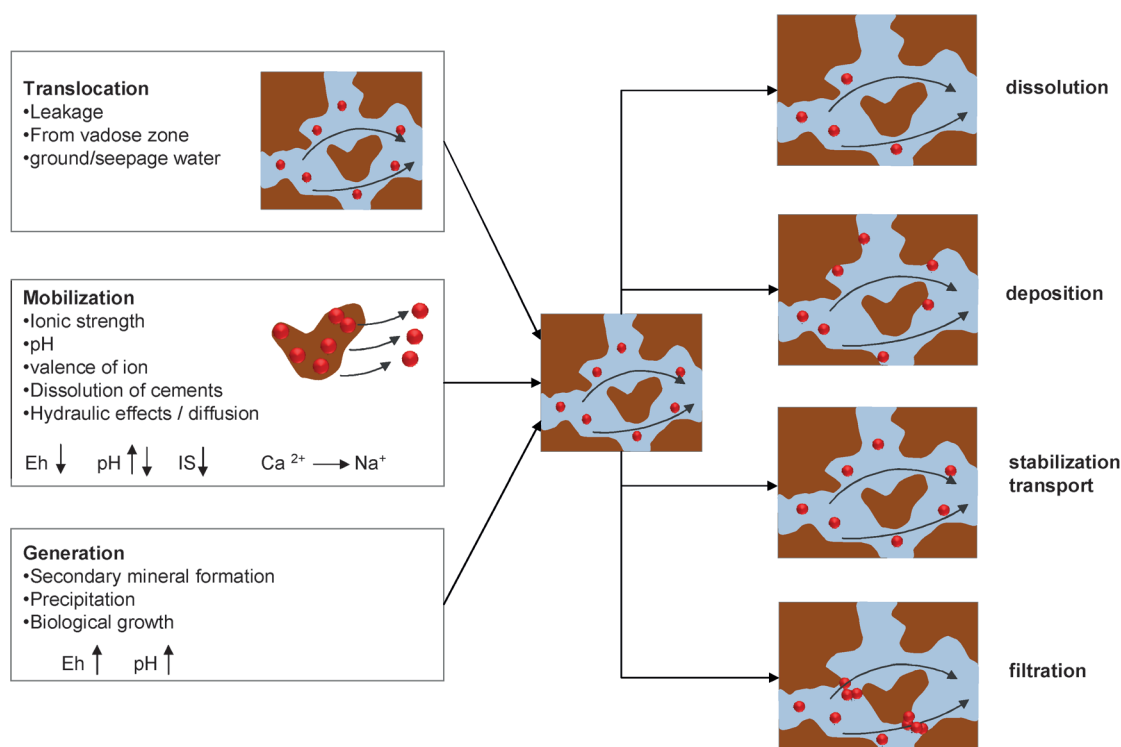


Figure 6. Particle transport processes in saturated porous media (adapted from McCarthy and Zachara<sup>[86]</sup>).

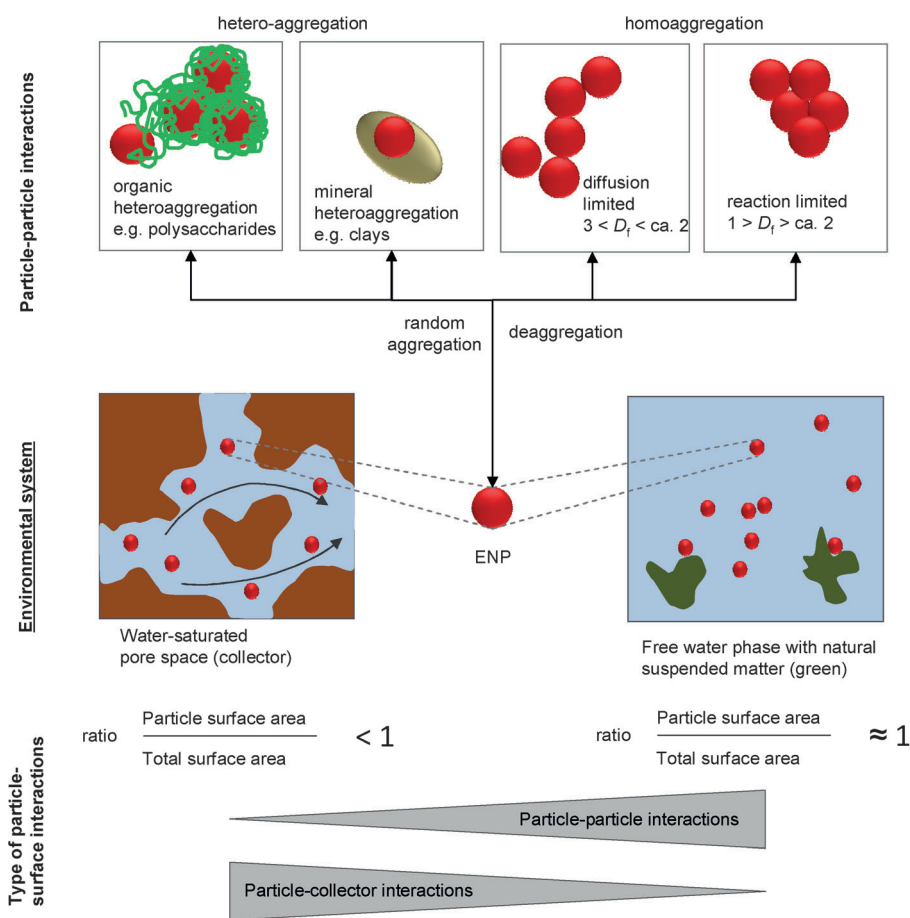


Figure 7. Particle aggregation processes in aqueous media, for example, pore space.

process for small particles (< 300 nm) and it determines the perikinetic aggregation rate. A particle suspension is always thermodynamically unstable and aggregation takes place as a result of particle-particle collision. Not every collision leads to aggregate formation because of repulsive forces between the particles. The origin of repulsive forces between particles can be electrostatic. Electrostatic interactions are attributed to the electrical double layer (EDL), which carries either a negative or a positive net charge, and are repulsive between similar surface charges. If the net charge is partially neutralized by increasing the ionic strength, the EDL will be compressed and the height of the energy barrier is affected. Particles can approach closer to each other and attractive forces acting on a shorter length scale, such as van der Waals interactions, might destabilize the particle suspension. Essentially, the height of the energy barrier between the particles controls the aggregation as well as the deposition. Assuming there is an increasing salt

concentration, there will be a limit (critical coagulation concentration, CCC) where the particles are completely destabilized and the aggregation rate reaches its maximum (each particle–particle collisions results in attachment). A further increase in the aggregation rate by increasing the salt concentration is not possible because each collision results in attachment and the collision rate is limited by diffusion. These processes are combined in the DLVO theory, which balances the attractive (van der Waals) and repulsive (electrostatic) forces acting on two particles.<sup>[91]</sup> Other interactions, such as hydrophobic interactions, steric repulsion, polymer bridging, magnetic, and hydration effects, might affect the aggregation/deposition and are termed non-DLVO processes.<sup>[89]</sup> Steric stabilization by surface orientation, binding of surfactant molecules, or polymers might overcome the attractive forces, thus causing a stabilization of the particle suspension.

In addition to aggregation, there are a number of other processes, such as deposition, which control the mobility of particles in porous media.<sup>[88b]</sup> Deposition is, similar to aggregation, controlled by the charge properties and steric effects between two surfaces. Physical entrapment (straining) is described as particle retention because of the size of the particles and the size of the pores, despite the solution chemistry being favorable for transport. It has been suggested that down-gradient pore throats are too small to allow particle passage, which is typically observed for CNTs (see Ref. [92] and references therein). Size exclusion, where large particles or particle aggregates are excluded from small pore spaces and can only be transported through larger pores, can certainly be relevant for colloids and ENPs.<sup>[88a,93]</sup> For an improved understanding and prediction of the transport behavior of natural colloids in porous media and surface waters, it is important to know which key environmental factors, such as pH value, ionic strength, and dissolved organic matter, control their surface charge and surface chemistry. Most of the available data for this purpose were obtained in laboratory experiments under well-defined conditions. However, a direct comparison of the data is not possible because of variations in the boundary conditions, which were not unified among studies. The transfer of the information from the laboratory to field conditions is not possible. Therefore, there is an increasing number of studies which focus on simulating natural conditions (e.g. studies on heteroaggregation).<sup>[90]</sup> Differences in the behavior of natural colloids and ENPs will be identified on the basis of the available process-oriented understanding, and applied to environmental conditions.

#### 4.2. Key Environmental Factors Affecting Aggregation and Deposition

The key environmental factors that control the colloidal stability are pH value, ionic strength, electrolyte valence, and particle coating.<sup>[33c]</sup> The pH value of a solution controls the surface charge of the particles. Kretzschmar et al. observed fast coagulation of natural kaolinite clay particles at pH < 5.8. A significant reduction in the coagulation occurred at pH values above 5.8, which is close to the point of zero

charge (PZC).<sup>[85]</sup> The net charge is positive when the pH values are lower than the PZC, which results in electrostatic attractive forces. At higher pH values, electrostatic stabilization is introduced by negatively charged surfaces. In the presence of humic acid (HA), negatively charged surfaces can also occur at pH values below the PZC, thereby reducing the coagulation. At an ionic strength  $\leq 0.01$  M, the stabilizing effect of adsorbed HA can be attributed solely to electrostatic interactions, that is, that aggregation behavior can be predicted by the DLVO theory. The aggregation behavior of kaolinite clay colloids depends on the pH value, ionic strength, and presence of HA. The mobility of hematite colloids was found to increase as the HA concentration increased (Figure 8).<sup>[1]</sup>

The pH dependency of the aggregation and deposition of engineered iron nanoparticles was demonstrated, for example, by Baalousha et al.<sup>[94]</sup> These materials acted according to the predicted behavior based on their point of zero charge (PZC). The PZC is not only material-specific, but depends on a number of additional factors. For oxide surfaces, such as Goethite, it is 7.4–9.5. The PZC of TiO<sub>2</sub> particles was determined to be between 4.2 and 6.3.<sup>[96]</sup> The case-specific

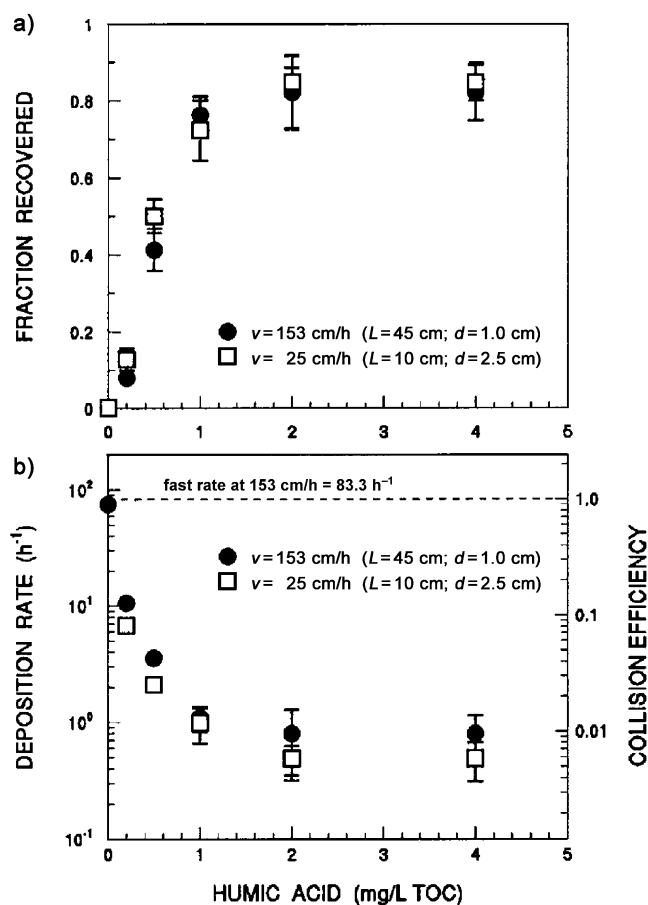


**Figure 8.** Influence of humic acid on the transport and deposition kinetics of hematite colloids in a sandy soil. a) Fractions of colloids that were recovered in the column effluents. Different column dimensions were used to achieve measurable colloid breakthrough peaks ( $L$ : column length;  $d$ : column diameter). b) Corresponding colloid deposition rate coefficients at two different water flow velocities (adapted from Kretzschmar and Sticher).<sup>[1]</sup> TOC = total organic carbon.

PZC of iron oxide material was determined to be pH 9.1.<sup>[94]</sup> Zeta potential measurements suggest that iron oxide NPs are highly positively charged at pH values between 2 and 6. In agreement with the theory, only a slight increase in the NP size was observed as the pH value was increased from 2 to 6. A more pronounced increase in size is reported at pH values >6. The maximum is reached at pH 8.5. The zeta potential decreases with an increase in pH value from 6 to 9 and becomes negative at pH 10. This observation agrees well with the described DLVO theory. It predicts pronounced aggregation close to the point of zero charge for bare NPs. In most studies it was demonstrated that ENPs such as bare metal and metal oxides behave similarly to natural colloids.<sup>[89]</sup> The behavior of coated ENPs may also be affected by changes in the pH value because functional groups of the coating, for example, carboxy groups, can be either protonated or deprotonated at a certain pH value. Additionally, the surface charge below the coating is also affected by changes in the pH value of the aqueous bulk solution, as was observed by Kim et al. for nZVI particles.<sup>[97]</sup> This might lead to enhanced aggregation and deposition, even of coated ENPs.

The solution composition, that is, the type and concentration of anions and cations in solution is an additional factor that affects the surface charge and surface potential. Three effects can be observed as the ionic strength increases: I) suppression of the electrical double layer, II) decrease in the zeta potential, and III) changes in the charge at the nanoparticle surface because of counterion adsorption. The specific adsorption of ions onto the NP surface (III) can modify the surface charge of a particle, even if the ionic strength does not change. As demonstrated for natural colloids, the ionic strength and the type of electrolyte significantly influence the aggregation behavior of NPs (see Ref. [89] and references therein). The change in the surface charge density causes a shift in the zeta potential, which might lead to destabilization of the particles. It is even possible that charge reversal occurs if sufficient specifically adsorbing ions are available. Charge reversal and neutralization might result in a destabilization of the particles.<sup>[98]</sup> The sedimentation and aggregation of negatively charged AuNPs was enhanced by elevated water hardness

(or ionic strength).<sup>[99]</sup> In accordance with theory,<sup>[100]</sup> an increase in the ionic strength (IS) generally resulted in the aggregation of bare TiO<sub>2</sub> particles. The size of the TiO<sub>2</sub> particles, which had an initial diameter of 50–60 nm, quickly increased up to the micrometer range after elevating the IS from 4.5 mM to 16.5 mM in a NaCl solution (pH ≈ 4.5). The effect of increasing ionic strength on different ENPs and natural colloids is similar, and CCCs for both groups are in a comparable range (Figure 9).

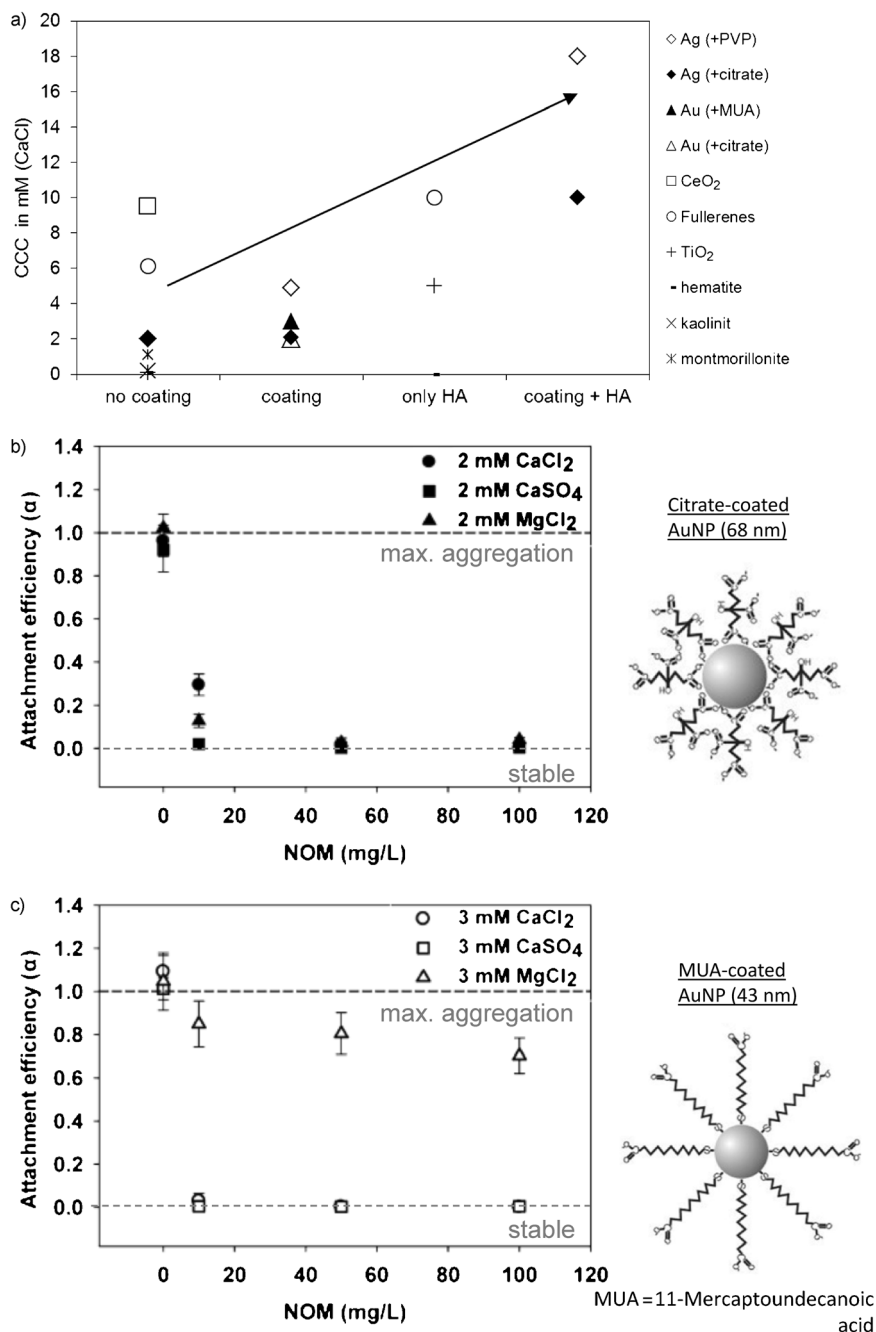


**Figure 9.** a) Critical coagulation concentrations (CaCl<sub>2</sub>) for ENMs and natural colloids/NPs with different electrolytes and organic coatings. Ag: Huynh et al. (2013); Au: Liu et al. (2013); CeO<sub>2</sub>: Li et al. (2011); fullerenes: Chen and Elimilech (2007); TiO<sub>2</sub>: Thio et al. (2012); Hematite: Kretzschmar et al. (1997); Kaolinit: Swartzen-Allen et al. (1976). b,c) Influence of SRNOM on the fast aggregation of citrate- and MUA-coated Au NPs by divalent electrolytes (adapted from Liu et al.<sup>[101]</sup>).

Mixtures of cations and anions have an additive effect on the aggregation kinetics, and the effect is controlled by the dominant ion.<sup>[102]</sup> French et al. demonstrated that, under similar pH and ionic strength conditions, the aggregation of TiO<sub>2</sub> NPs was faster if CaCl<sub>2</sub> was present as an electrolyte compared to in the presence of NaCl.<sup>[103]</sup> Divalent cations have, in general, a stronger influence on the aggregation of negatively charge ENMs compared to monovalent ions.<sup>[33c,98,101,102,104]</sup> This effect is caused by the adsorption of cations to negatively charged surfaces. The destabilizing effect of cations is in the order  $\text{Ca}^{2+} = \text{Mg}^{2+} \gg \text{Na}^+$  for the aggregation of citrate and Au NPs coated with 11-mercaptoundecanoic acid (MUA).<sup>[101]</sup> The aggregation of single-wall carbon nanotubes can be induced by an increase in the salt concentration and by adding divalent calcium ions. The electrostatic charge is reduced and thereby the electrostatic repulsion suppressed, which is similar to observations with aquatic colloidal particles.<sup>[105]</sup> This finding demonstrates that DLVO theory can generally explain the aggregation behavior of bare NPs, such as TiO<sub>2</sub> NPs,<sup>[98]</sup> ZnO NPs,<sup>[106]</sup> or CeO<sub>2</sub> NPs,<sup>[107]</sup> as it is applied for natural colloids. The stability and transport of NPs coated with an organic layer was very often not predictable by DLVO theory and deviates from that of uncoated particles. Electrosteric stabilization causes an increased mobility compared to bare NPs.<sup>[36b,106,107]</sup> In general, it was concluded that the coating has a stronger impact on the ENP behavior than the core material.<sup>[108]</sup> An organic coating at the particle surface affects the aggregation behavior and increases the CCC (Figure 9). A similar effect was observed for the presence of NOM.

Natural organic matter (NOM), as a diverse compound group in aqueous environments, affects the surface chemistry of particles not solely in terms of charge and surface potential but also in terms of the structure (steric orientation). Numerous studies have reported that NOM has the ability to stabilize a variety of organic and inorganic materials, such as natural colloids. It is similar to a weak acid and, therefore, anionic at neutral pH values. Kretschmar et al. reported a decrease in the collision efficiency of natural colloids with increasing HA concentrations in column transport experiments.<sup>[1]</sup> Similar behavior was observed for ENMs in contact with NOM. In general, the adsorption of NOM on hydrophilic surfaces is pH-dependent and stronger for a positively charged particle surface under conditions where  $\text{p}K_{\text{a,DOM}} < \text{pH}$ .<sup>[109]</sup> The anionic organic material is adsorbed onto the surface, thereby causing a rather low negative zeta potential. It was also reported that NOM may neutralize or even reverse the charge of NP surfaces.<sup>[94]</sup> In the case of charge reversal of positively charged colloids, heteroaggregation with negatively charged soil minerals would be inhibited.<sup>[110]</sup> However, the stability of such colloids is often higher than predicted by the zeta potential and it is believed that steric stabilization plays a major role. At high ionic strength or low pH value, in particular, the compressed double layer of natural iron colloids allows interactions which are controlled by steric repulsion between the NOM coatings.<sup>[106]</sup> Sufficiently high NOM concentrations are required for the most pronounced effects.<sup>[41b,45d,94,101,111]</sup> According to Chen et al., electrostatic stabilization is promoted at low HA concentration, and

a combination of electrostatic and steric stabilization enhances the stability of ENPs as the HA concentration increases.<sup>[109]</sup> It is known that besides the NOM concentration, the composition of the NOM has an impact on the stability of colloids. An enhanced stability of ZnS nanoparticles was observed as the aromaticity and molecular weight of the NOM increased, which is responsible for more pronounced electrosteric hindrance between particles.<sup>[45d]</sup> Furman et al. reported that HA reduces the deposition of AgNPs onto silica surfaces more effectively than the fulvic fraction, which has a lower molecular weight than HA.<sup>[112]</sup> The prediction of aggregation and deposition of ENPs in natural systems requires that the combined effects of HA and elevated ionic strength conditions are accounted for.<sup>[113]</sup> Specific or electrostatic interactions between the NOM, electrolyte, and particle coating might influence the aggregation behavior significantly.

If the ENPs are initially coated by an organic substance, then interactions with the NOM have to be taken into account. The extent of the interaction between the NOM and ENP coating are strongly related to the type of coating and its interactions with the particle surface (see Ref. [44] and references therein). It is, therefore, a major controlling factor for the aggregation and deposition behavior, as proved by a number of studies.<sup>[108,114]</sup> A citrate coating of Au NPs was partially substituted or over-coated by HA, thereby causing an increase in the stability at low pH values because of steric stabilization.<sup>[115]</sup> Strong coagulation as a result of the presence of Ca<sup>2+</sup> might be inhibited in the presence of NOM, which is not in accordance with DLVO theory.<sup>[101]</sup> Figure 9 depicts the importance of the type of coating on the aggregation behavior of ENPs. Au NPs coated with covalently bound MUA are not stabilized in the presence of NOM if Mg<sup>2+</sup> ions are in solution. A stabilizing effect of the NOM was, however, observed for citrate-coated Au NPs. Liu et al. hypothesized that Mg<sup>2+</sup> ions have a lower affinity to the carboxy groups of MUA and, therefore, cannot act as a bridging agent between the MUA and NOM. This causes fewer interactions between the NOM and the surface coating, and the suspension stability cannot be increased by the presence of NOM. Another possibility is that the MUA coating cannot be replaced by HA, and Mg<sup>2+</sup> is less complexed by the free HA molecules because of the weaker interaction with carboxylic groups. Therefore, the free Mg<sup>2+</sup> activity remains higher compared to that of Ca<sup>2+</sup>, and leads to the aggregation of the unchanged particles. This behavior clearly contradicts the expectations derived from natural particles.<sup>[101]</sup>

Commercial coatings might prevent homoaggregation, but not necessarily heteroaggregation.<sup>[116]</sup> The type of NP coating influences the stability of nanomaterials significantly.<sup>[33c,117]</sup> Not only the aggregation behavior, but also the deposition behavior is widely influenced by the coating of the NPs.<sup>[114b,118]</sup> Phenrat et al. proved by applying empirical correlations for electrostatically stabilized NPs that the deposition of polymer-coated NPs was overestimated.<sup>[114b,118]</sup> These correlations did not take into account electrosteric repulsion and the decrease in friction caused by such coatings. There are only a few studies which point out that the organic

coating does not affect the fate and behavior of ENPs, for example, PVP-coated Ag NPs in sewage.<sup>[32b]</sup> These observations are explained by degradation or desorption of the organic coating, which is discussed Section 3.

### 4.3. Quantitative Descriptors for Aggregation and Deposition

Particle stability and mobility in surface waters and in porous media are strongly related to the aggregation and deposition of the nanoparticles, respectively. There are detailed modeling approaches for aggregation. This section focuses on elucidating the most common approach to quantitatively describe particle stability. Particle mobility in porous media is only touched on here. The particle–particle collision frequency is controlled by the temperature and the particle number concentration. If the suspension is completely destabilized, each particle collision results in attachment. The ratio between particle collisions resulting in attachment and maximum possible attachments is defined as the attachment efficiency. The attachment efficiency  $\alpha_a$  under destabilizing conditions is equal to 1. However, the aggregation rate constant under certain environmental conditions might not reach its maximum, thereby resulting in  $\alpha_a < 1$ . The aggregation rate of a suspension is described by Equation (1), where  $k_a$  is the second-order rate constant,  $n$  is the number concentration in the suspension, and  $\beta$  is the mass transport coefficient.

$$\frac{dn}{dt} = k_a n^2 \text{ with } k_a = \alpha_a \beta \quad (1)$$

If there is no energy barrier, and the aggregation is solely controlled by diffusion, the rate constant is expressed by the Smoluchowski Equation [Eq. (2)], where  $k_B$  is the Boltzmann constant,  $T$  is the temperature in  $K$ , and  $\eta$  is the dynamic viscosity.

$$k_a = \frac{4k_B T}{3\eta} \quad (2)$$

This rate equals the maximum aggregation rate. If an energy barrier exists, a slower aggregation rate would be expected and the mass-transport coefficient has to be considered. This case has to be expected for natural aquatic systems. The determination of the mass-transport coefficient  $\beta$  for aggregation has been further discussed by Buffle and van Leeuwen.<sup>[119]</sup> A commonly applied approach is based on the concept of the stability ratio,<sup>[119]</sup> which is the inverse of the aggregation attachment efficiency  $\alpha_a$  [Eq. (3)]. Here,  $k$  is the inverse Debye length,  $a_p$  the particle radius,  $V_{\max}$  the energy barrier height, and  $T$  the absolute temperature.

$$W = \frac{1}{\alpha_a} \approx 2ka_p \exp\left(-\frac{V_{\max}}{k_B T}\right) \quad (3)$$

The aggregation rate constant for small and larger particles is similar because small particles have a higher diffusion coefficient but large particles a larger collision radius. It can be deduced from the Smoluchowski Equation

for perikinetic aggregation rates that the aggregation rate constants for spherical particles of different sizes is larger than those of particles of the same size. Therefore, the aggregation rates of engineered NPs in aquatic environments might be higher in the presence of larger natural colloids compared to homoaggregation processes.

Particle deposition is especially relevant for particle mobility in the pore space of groundwater aquifers. Factors controlling the collision efficiency are similar to aggregation. Therefore, the mobility in porous media is limited under conditions favoring aggregation.<sup>[114a]</sup> There are a number of quantitative tools for modeling the transport behavior of ENMs and natural colloids. All are based on the general description of the process by Equation (4), where  $L$  is the distance along the length of the porous media, and  $k_d$  is the first order rate constant.

$$\frac{dn}{dL} = k_d n \quad (4)$$

The attachment efficiency defined in filtration theory can be calculated as described by Tufenkji and Elimelech<sup>[120]</sup> as well as Cornelis et al.<sup>[88a]</sup>

### 4.4. Comparison of the Stability and Mobility of ENPs and Natural Colloids

The stability and mobility of particles in aqueous environments are controlled by the particle number concentration, the charge, and the structure of the particle surface. The most relevant key environmental factors controlling their stability are pH value, ionic strength, and NOM, with the pH value and ionic strength affecting the surface charge, and the NOM the steric particle–particle interactions.<sup>[114b]</sup> It was demonstrated that the surface charge of ENPs is similarly affected by the key environmental factors as natural colloids.<sup>[89,100,121]</sup> The current state of knowledge supports the hypothesis that the fate and behavior of bare ENPs is similar to their natural counterparts.<sup>[102,106,114a,122]</sup> Only the presence of persistent organic coatings introduces particle properties which differ from the core material in terms of stability and mobility. Such coatings do not exist with natural colloids, and this clearly differentiates the fate of organically coated ENPs and their natural counterparts. However, there are only a few examples which exhibit a distinct behavior (e.g. PVP-coated ENPs). Nowadays, materials with such coatings can be found in very specific applications such as pharmaceuticals. However, such products are still in development, and when there is an application it is commonly locally restricted in a controlled environment (hospitals, electronic industry). The prediction of the behavior of ENPs coated with a persistent organic material is based on empirical approaches because DLVO does not consider, amongst other things, steric interaction. Such predictions have to date not provided reliable results. Therefore, process-based models are required to perform adequate prediction, which are compulsory for safety research and hazardous assessment.

## 5. Dissolution

Nanoparticles are, unlike the bulk materials, metastable and are, therefore, likely to undergo growth in supersaturated conditions or dissolution in under-saturated conditions.<sup>[123]</sup> The former process is of relatively low importance in terms of environmental fate, because the chance that engineered nanomaterials enter natural waters which are supersaturated in terms of the particles' components is rather small. In contrast, dissolution is one of the major potential pathways that nanomaterials can follow in the environment and may lead to full depletion of the solid phase and/or the precipitation of new chemical structures (Figure 10). It is an important process for the release of not only the constituents of a particle, but also other species that may have co-precipitated or adsorbed on the particles' surface.<sup>[124]</sup> As with all chemical reactions, the driving force for dissolution is a reduction in the total Gibbs energy of the solid/liquid system. Dissolution is typically expressed by the solubility constant of the particles' constituents; however this value refers to equilibrium conditions and does not include information on the transport phenomena between the solid and liquid phases that may affect dissolution kinetics, for example, space confinement as a result of aggregation<sup>[125]</sup> and the adsorption of complex organic compounds that may reduce the diffusion of molecules between a particle's surface and its surrounding solution.

Dissolution is controlled by a number of particle- and solution-specific properties: 1) the solubility constant, 2) chemical speciation (e.g. acid–base reactions, complexation, re-precipitation), and 3) the specific surface area and mass-transfer kinetics.<sup>[126]</sup> Solubility (1) is a thermodynamic property that refers to equilibrium conditions and is influenced by the surface strain, crystallinity, and crystal phase, the presence of structural anomalies, particle size, and temperature. Overall, higher solubility is expected for small particles with low crystallinity or irregularities on their surface

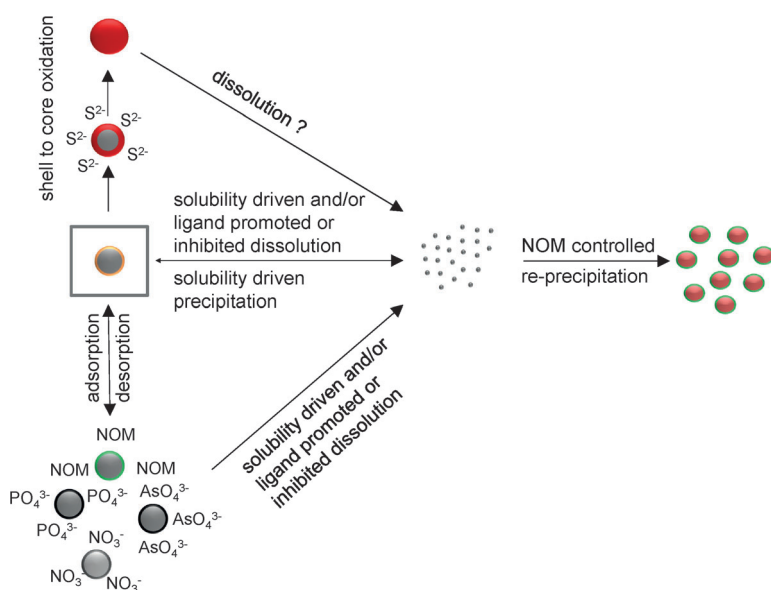


Figure 10. a) Possible processes involved in the dissolution of ENPs.

(cavities, bumps, interfacial borders). Dissolution is often a reversible reaction (dissolved metal ions may re-precipitate on the solid surface) and, therefore, the chemical speciation (2) of dissolved constituents may enhance the dissolution by depletion of the free metal ions. Finally, dissolution is a surface reaction and is highly dependent on the available surface area and (often diffusion-controlled) mass transfer (3) between the surface and the bulk solution. As dissolution is dependent on the specific surface area, dissolution rates are often reduced by aggregation, attachment, and surface coverage by adsorbed organic compounds (e.g. engineered coatings or NOM).

The majority of studies on the dissolution of engineered nanomaterials have focused on silver and to a lesser extent on ZnO. In the case of metallic silver, oxidation by dissolved oxygen is the rate-limiting step, and dissolution rates were found to decrease as the dissolved oxygen concentration decreased, by the addition of natural organic matter, a reduction in temperature, or an increase in the pH value.<sup>[127]</sup> Dissolution of zero-valent metals requires an oxidation step and is, therefore, more complex than the dissolution of metal oxides. For example, ZnO readily dissolves in moderately hard water.<sup>[128]</sup> Dissolution studies of naturally occurring nanomaterials have focused on iron oxides, because of their natural abundance, while other metal oxides (e.g. CuO) have also been studied. In the previous sections we compared the transformation, aggregation, and deposition potential of engineered nanomaterials to their naturally occurring counterparts. However, there is a large body of information available on the dissolution of bulk materials and it seems more appropriate to compare nanomaterials (engineered or natural) with their respective bulk materials in terms of dissolution processes and dissolution products. In other words, if the dissolution process and products of nanomaterials do not differ from what is already known for their bulk counterparts, there is no need for further research on the dissolution behavior of every nanomaterial and coating that is available in the market. Therefore, it is essential to determine those material properties that cause significant deviation of the dissolution potential from that of the bulk material (e.g. surface strain, resistant coatings, etc.).

### 5.1. Solubility

The solubility of a particle with known radius can be calculated from the solubility of the bulk material by using a modified form of the Kelvin Equation [Eq. (5)].<sup>[129]</sup> Here,  $S$  is the solubility,  $\gamma$  is the surface tension of the particle,  $V_m$  is the molar volume,  $R$  is the gas constant,  $T$  is the temperature, and  $r$  and bulk indicate the solubility of a particle with radius  $r$  and the bulk material, respectively.

$$S_r = S_{\text{bulk}} \times \exp\left(\frac{2\gamma V_m}{RT r}\right) \quad (5)$$

This calculation, however, is only possible when the surface strain of the nanomaterial, defined as the set of relative displacements of surface atoms from their positions prior to energy minimization, is the same as in the bulk material. The surface strain of silver nanoparticles as small as 5 nm was found to be the same as that of bulk silver,<sup>[129a]</sup> which is consistent with the similarity of the surface-area-normalized dissolution rates measured for nano and bulk silver (Figure 11).<sup>[56b]</sup>

However, that is typically not the case for particles smaller than 20–30 nm, where the atomic structure on the surface is especially distorted.<sup>[130]</sup> Echigo et al. studied the reductive dissolution of hematite and demonstrated that surface defects are responsible for the enhanced dissolution rate of 30 nm rhombohedral crystals, while aggregation is responsible for the decreased dissolution rate of 7 nm pseudohexagonal plates, even though the surface-normalized initial dissolution rate of the latter was higher than the former by a factor of almost two.<sup>[58c]</sup> Furthermore, amorphous structures are less stable than crystalline phases with lower density and higher surface strain (Figure 12, compare crystalline P25 and amorphous TIPO TiO<sub>2</sub> particles), and are much more prone to dissolution than crystalline material.<sup>[123]</sup> Solubility, as depicted in Figure 12, is also affected by solution chemistry such as the pH value and the presence of other ions in solution (e.g. Cl<sup>-</sup>).

The ratio  $S_i/S_{\text{bulk}}$  may be a useful tool for predicting the fate of nanomaterials in terms of their tendency to dissolve. Measurements of the surface tension are needed to determine the solubility; however such measurements are technically challenging and are rarely reported.

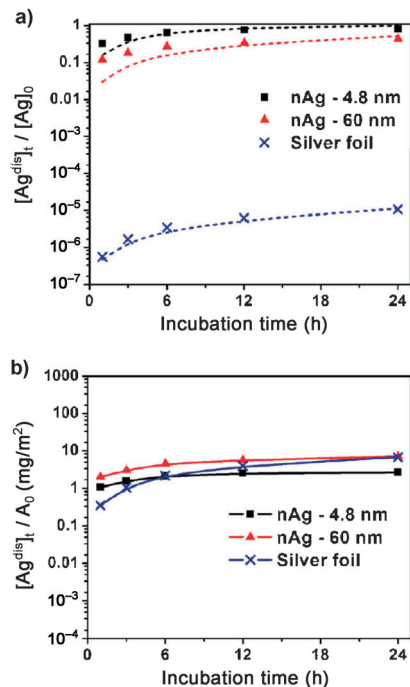


**Figure 11.** a) Time-resolved mass-based measurements of the release of soluble silver in air-saturated acetate buffer (pH 4),  $[Ag]_0$  is the total silver atom concentration (all forms) in the system. b) The same release of soluble silver as in (a) but normalized to the surface area (adapted from Liu et al.<sup>[56b]</sup>).

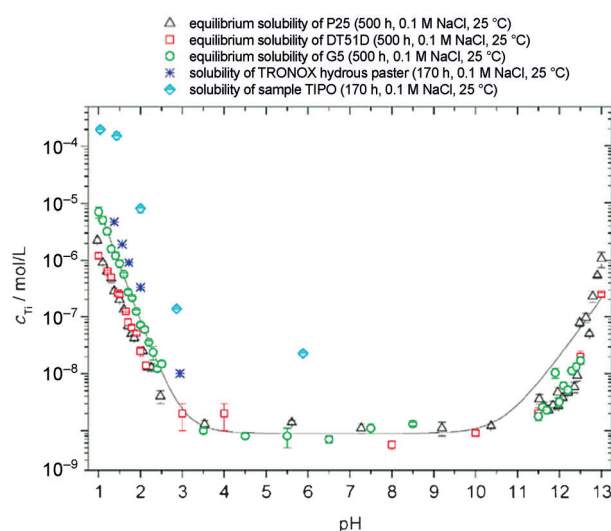


**Figure 12.** Solubility of crystalline titania (P25, DT51D, G5) and amorphous titanium hydrous oxides (TRONOX, TIPO) as determined by AdSV, and their dependence on the pH value ( $0.1 \text{ mol L}^{-1}$  NaCl; 25 °C). Solid line: solubility of titanium dioxide ( $I=0.1 \text{ mol L}^{-1}$ ; 25 °C) calculated with the equilibrium constants determined in this study (from Schmidt and Vogelsberger<sup>[131]</sup>).

## 5.2. Solution Chemistry and Kinetics

Solubility may provide useful information about the tendency of a material to withstand weathering, but it refers to equilibrium conditions that are unlikely to be reached in natural systems. Kinetic effects need to be considered in the context of environmental fate. Dissolution rates are influenced by several parameters, such as pH value, specific surface area, hydrochemistry (especially concentrations of ligands in the solution), and the adsorption of organic or inorganic compounds. As a result of their complexity, empirical models are usually employed to describe dissolution kinetics. The solution hydrochemistry dictates the chemical speciation of dissolved species and thus exerts a significant amount of influence on dissolution processes. The complexation or precipitation of atoms dissolving from a solid surface leads to a reduction in the concentration of the free dissolved species and drives the dissolution of more atoms from the solid phase, thus favoring dissolution. The higher the concentration and variety of ligands which are able to bind free species present in solution, the faster the dissolution of the solid surface. For example, the dissolution of silver nanoparticles is enhanced when the free silver ions bind to sulfur-,<sup>[67b]</sup> chloride-,<sup>[132]</sup> amine-,<sup>[133]</sup> or thiol-containing organic compounds.<sup>[49]</sup> Similarly, the dissolution of goethite particles is enhanced by oxalate.<sup>[134]</sup>

An empirical kinetic law has been derived by Liu and Hurt that takes into account the thermodynamic and hydrochemical parameters that affect the dissolution of nano-Ag, namely temperature, pH value, concentration of the NOM, and the concentration of silver, as shown in Equation (6).<sup>[127]</sup> Here,  $m$  is the concentration of particulate silver,  $T$  is the temperature,  $[NOM]$  the concentration of natural organic matter, and constants  $A$ ,  $E$ , and  $a$  are parameters that were

calculated after fitting the above equation to experimental data.

$$-\frac{1}{m} \frac{dm}{dt} = A e^{-E/RT} \left( \frac{[H^+]}{10^{-7} M} \right)^{0.18} e^{-a[NOM]} \quad (6)$$

Such empirical equations may be very useful for comparing dissolution kinetics and depletion of the nanomaterials from other processes, such as aggregation, deposition, and surface transformation reactions.

Dissolution rates are also proportional to the available surface area. It has often been observed that aggregation leads to reduced dissolution rates, possibly because of a decrease in the reactive surface area (e.g. see Ref. [129b]). A reduction in dissolution rates has also been observed between nanomaterials with adsorbed synthetic coatings or natural organic compounds. The driving force for adsorption is the reduction of the surface free energy (the same holds true during crystal growth). Coverage of the particles' surface by the adsorbed compounds reduces the total free energy of the surface and results in partial isolation of the solid from its surrounding solution. The extent and persistence of this isolating layer is a function of the surface complexation between the organic and the surface ions (inner- or outer-sphere complexation) and the hydrophobicity of the organic material. However, ligands may not only adsorb on the nanomaterial surface, but also enhance its dissolution. Ligands that bind specifically on metal atoms on the surface of nanomaterials may be present in the water medium or as engineered coatings on the original nanomaterial, and their effect on dissolution necessitates further research and needs to be incorporated in empirical dissolution models. Important parameters for the dissolution of materials are the pH value, concentration of NOM, and the presence of specific-binding ligands.<sup>[128]</sup> Liu and Hurt developed an empirical model that predicts dissolution rates of Ag ENMs under these conditions.<sup>[127]</sup> Dissolution rates of ENMs are also affected by engineered organic coatings. For example, Gondikas et al. observed that PVP-coated Ag ENMs dissolved more slowly than citrate-coated ones.<sup>[49]</sup> Parameters such as the organic coating material were also observed not to affect the solubility.<sup>[129a]</sup>

### 5.3. Comparison of the Dissolution Behavior of Engineered and Natural Particles

Experiments conducted in environmentally relevant systems (e.g. mesocosms, microcosms, or simulated wastewater treatment plants) have shown that metal-containing nanoparticles may undergo several modifications in the environment. For example, silver nanoparticles have been detected as silver sulfides, silver chlorides, or silver-NOM complexes, which can be thought of as metabolites of the original particles.<sup>[47,63,64]</sup> These reported differences between the original and the modified material may be a result of surface modifications or dissolution followed by re-precipitation of the dissolved species. The former case is addressed in Section 3. The dissolution of nanomaterials can result in the

precipitation of structures that would not occur in an over-saturated system or in a system where there is re-precipitation after dissolution of bulk materials. For example, ZnO nanowires have been shown to dissolve and re-precipitate as ZnCO<sub>3</sub> nanowires.<sup>[135]</sup> Silver nanoparticles dissolve in the presence of inorganic ligands such as chloride and sulfur, and re-precipitate as AgCl or Ag<sub>2</sub>S NPs;<sup>[67b,73]</sup> in the latter case, dissolution and re-precipitation leads to aggregates that consist of nanoparticles linked through "nano bridges" of silver sulfide. At low sulfur to silver molar ratios, silver first dissolves to form silver ions, which then precipitate as silver sulfide.<sup>[66]</sup> The same process leads to the re-precipitation of nano-ZnS after dissolution of nano-ZnO.<sup>[136]</sup> The dissolution and re-precipitation of nanomaterials are important processes that influence the transport and bioavailability of metals in the environment<sup>[46b]</sup> and are heavily regulated by the NOM.<sup>[44]</sup> Recent studies have shown that specific properties of the NOM and the presence of metal-binding ligands are primarily responsible for this effect.<sup>[45d,137]</sup> These products are unique for nanoparticles and their formation mechanisms require further examination. A more complex process takes place in biological systems, where it is hypothesized that silver nanoparticles undergo complete dissolution in the GI tract of the human body to form organo-Ag complexes, which are circulated through the body and can be photoreduced on skin areas, where they deposit as secondary silver nanoparticles.<sup>[138]</sup> Similar processes may take place with organo-Ag complexes formed in the environment during exposure of plants to nano-Ag and the subsequent release of organic compounds from the plants as a response mechanism.<sup>[40]</sup> This mechanism, however, is unlikely to differ between ionic, nano, and bulk silver. In addition, the case of dissolved metal species (catalyst residues) leaching from carbon nanotubes<sup>[69a]</sup> can be thought to be similar to that of metal ions desorbing from a solid surface. This would not hold true if the catalyst residues were partially released in the form of nanoparticles, as has been shown for nickel in single-wall carbon nanotubes.<sup>[139]</sup>

## 6. Summary and Conclusions

### 6.1. Current State of Knowledge

To find an answer to the question of whether the release of ENMs in aqueous environments causes risks, information on fate and behavior are essential. The increasing production and application of ENMs means that they are released into the environment, in some recent cases the amounts were quantified.<sup>[6]</sup> Quantification of ENM release and environmental concentrations is hampered by high uncertainties because of the lack of reliable data regarding production volumes and the lack of ENM-specific monitoring techniques for complex matrices such as surface or waste waters. Despite the uncertainties of the available data, it can be concluded that the PECs of engineered materials remain orders of magnitudes below the environmental concentrations (ECs) of natural colloids.<sup>[31]</sup> Natural colloids are ubiquitous in aqueous environmental media. Their concentration in terms of mass

and number is subject to variations and depends on the type of environment, that is, river, surface, or ground water.

Regardless of the particle concentration, the fate and behavior of ENMs may differ compared to that of natural colloids. Processes such as surface transformations, stability, mobility, and dissolution control the fate and behavior. These processes are regulated by particle properties and the key environmental factors of pH value, ionic strength, UV radiation, NOM content, and NOM composition. Transformations of the particle surface in such environments might occur through degradation of the engineered organic coating, adsorption and desorption of organic or inorganic constituents, and redox reactions. Particle stability and mobility is a function of electrostatic and steric particle–particle interactions. By comparing the transformation of natural NPs and ENMs it was found that similar transformations can be expected when the core of the ENM has a natural counterpart. The mobility of ENMs which do not possess a persistent organic coating is regulated by similar key factors as the mobility of natural NPs, and the stability of both types of NPs is low. They tend to aggregate because of the high total number concentrations and the heterogeneity of the surface properties of natural colloids, which make them prone to heteroaggregation. Dissolution is likely in unsaturated conditions far from equilibrium, which is the case in most environmental systems. The solubility constant provides an indicator of the intensity of the thermodynamic driving force for dissolution; however, predicting dissolution rates requires experimental tests and the development of empirical equations. There are indications that re-precipitation plays a considerable role in the fate and behavior of ENMs. The presence of NOM is critical to the dissolution process and moderates the re-precipitation of minerals. ENMs with persistent engineered organic coatings and core–shell structures are expected to show distinct transformations and stability compared to natural particles.

### 6.2. A Decision Tree Model for Comparison between Engineered and Natural Nanomaterials

For the risk assessment of ENMs, the prediction of their fate and behavior in aqueous environments is of major relevance. Commonly applied thermodynamic models of dissolved water constituents are not applicable to colloidal systems. At present, predictions can only be derived from laboratory tests performed under relevant test conditions. However, such predictions have to challenge the critical transfer from natural-like conditions in the laboratory to the real environment. From the state-of-the-art knowledge, we developed a decision tree model for determining whether engineered nanomaterials are different to their natural counterparts in terms of their environmental fate (Figure 13). In cases where there is evidence of a distinct behavior, the model provides suggestions for laboratory tests which are

required to determine the fate and behavior of the specific ENM. The hydrochemistry of the aquatic system and the predicted or measured concentration of the ENMs are required as input parameters.

Secondly, it has to be determined whether naturally occurring particles exist with the same consistency and structure as the ENM under investigation. For example, metallic silver particles may also occur naturally from UV radiation of dissolved silver, while CdSe/ZnSe core–shell semiconducting nanoparticles are unlikely to be found in natural systems. When there is no natural counterpart for an ENM, who's predicted or measured environmental concentration may pose a risk to water quality or ecotoxicology, special research studies need to be carried out to determine their potential fate. In cases where natural counterparts exist and the ENMs have no engineered organic coating, or the coating is readily removed from the particle surface in the environment, there is no clear distinction between natural particles and ENMs. However, if the engineered organic coating is persistent for time scales that are relevant for the environmental fate of the ENMs, specific studies need to be carried out to determine their fate. These studies would include tests on surface modification, aggregation, and dissolution.

### 6.3. Perspectives in Risk Assessment of ENMs

Even though a wide range of studies have already been conducted for ENMs under environmentally relevant conditions, there are a few major drawbacks that require further analysis. First of all, realistic release levels are necessary to predict the environmental fate of ENMs. Secondly, aggregation studies in the vast majority of cases are focused on homoaggregation, that is, aggregation between particles of the same material. Given the much lower concentration of ENMs compared to the concentration of natural colloids and nanoparticles and the strong dependency of aggregation rates on number concentrations, heteroaggregation is much more likely to take place. However, the study of heteroaggregation

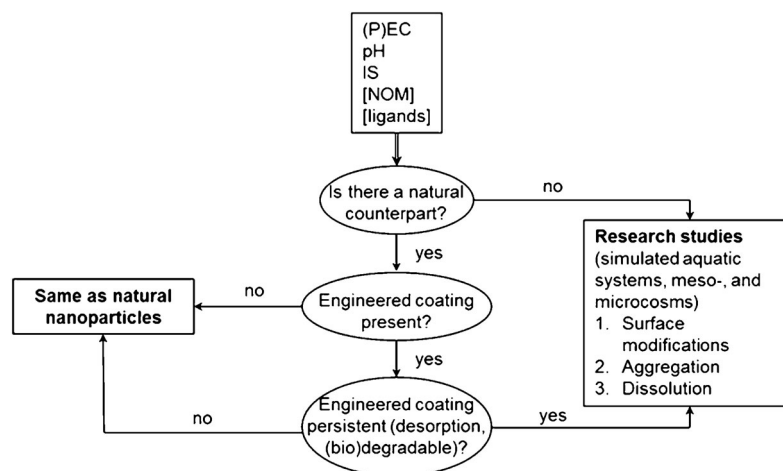


Figure 13. Schematic representation of the decision tree model.

is a very challenging task from a technical standpoint. Additionally, even though several studies have looked into the effect of the engineered coating type on the reactivity of the particles, there is relatively little information on the persistence of various engineered organic coatings on the particles surface under environmentally relevant conditions. Currently, the prediction of fate and behavior is based on experiments. It is envisaged that process-based models will be developed which will enable the user to predict the behavior and determine environmental concentrations under realistic scenarios. Finally, given the relatively recent technical advancements that allow us to study the nanoparticle fraction of colloid science, information on the importance of naturally occurring nanoparticles for the transport of organic and inorganic pollutants in natural waters should be revised, and further research is needed in that direction.

## 7. List of abbreviations

AdSV	adsorptive stripping voltammetry
CCC	critical coagulation concentration
CNT	carbon nanotube
$D_f$	fractal dimension
DLVO theory	a theory named after the researchers Derjagin, Landau, Verwey, and Overbeek
DOM	dissolved organic matter (in environmental chemistry, often interchangeably used with NOM)
EDL	electrical double layer
EDX	energy-dispersive X-ray analysis
ENM	engineered nanomaterial
ENP	engineered nanoparticle
FA	fulvic acid
FeOx	iron oxides, as a general term
HA	humic acid
IS	ionic strength
MUA	mercaptoundecanoic acid
NIOP	nano iron oxide particle
NOM	natural organic matter
NP	nanoparticle
nZVI	nanoscale zero-valent iron
PEC	predicted environmental concentration
PNEC	predicted non-effect concentration
PVP	polyvinylpyrrolidone
PZC	point of zero charge
RNIP	reactive nano iron particle(s)
STEM	scanning transmission electron microscope

*This work was supported by the DetectNano project supported by the Austrian Science Fund (FFG, no. 8357508) and the German Chemical Industry Association (VCI e.V.). We also acknowledge the support by Ricarda von der Kammer who provided us with the artwork for the frontispiece.*

Received: May 7, 2014

Published online: October 27, 2014

- [1] R. Kretzschmar, H. Sticher, *Environ. Sci. Technol.* **1997**, *31*, 3497–3504.
- [2] A. Hofmann, S. Thierbach, A. Semisch, A. Hartwig, M. Taupitz, E. Ruhl, C. Graf, *J. Mater. Chem.* **2010**, *20*, 7842–7853.
- [3] K. L. Plathe, F. von der Kammer, M. Hassellöv, J. N. Moore, M. Murayama, T. Hofmann, M. F. Hochella, *Geochim. Cosmochim. Acta* **2013**, *102*, 213–225.
- [4] F. Gottschalk, E. Kost, B. Nowack, *Environ. Toxicol. Chem.* **2013**, *32*, 1278–1287.
- [5] F. Gottschalk, B. Nowack, *J. Environ. Monit.* **2011**, *13*, 1145–1155.
- [6] F. Gottschalk, T. Y. Sun, B. Nowack, *Environ. Pollut.* **2013**, *181*, 287–300.
- [7] F. von der Kammer, P. L. Ferguson, P. A. Holden, A. Mason, K. R. Rogers, S. J. Klaine, A. A. Koelmans, N. Horne, J. M. Unrine, *Environ. Toxicol. Chem.* **2012**, *31*, 32–49.
- [8] M. Kah, P. Machinski, P. Koerner, K. Tiede, R. Grillo, L. F. Fraceto, T. Hofmann, *Environ. Sci. Pollut. Res. Int.* **2014**, *21*(20), 11699–11707.
- [9] N. C. Mueller, J. Braun, J. Bruns, M. Cernik, P. Rissing, D. Rickerby, B. Nowack, *Environ. Sci. Pollut. Res.* **2012**, *19*, 550–558.
- [10] a) M. Kah, S. Beulke, K. Tiede, T. Hofmann, *Crit. Rev. Environ. Sci. Technol.* **2013**, *43*, 1823–1867; b) M. Kah, T. Hofmann, *Environ. Int.* **2014**, *63*, 224–235.
- [11] N. Savage, M. S. Diallo, *J. Nanopart. Res.* **2005**, *7*, 331–342.
- [12] a) P. Hennebert, A. Avellan, J. F. Yan, O. Aguerre-Chariol, *Waste Manage.* **2013**, *33*, 1870–1881; b) A. L. Holder, E. P. Vejerano, X. Z. Zhou, L. C. Marr, *Environ. Sci. Proc. Imp.* **2013**, *15*, 1652–1664; c) C. O. Hendren, X. Mesnard, J. Dröge, M. R. Wiesner, *Environ. Sci. Technol.* **2011**, *45*, 2562–2569.
- [13] C. O. Hendren, A. R. Badireddy, E. Casman, M. R. Wiesner, *Sci. Total Environ.* **2013**, *449*, 418–425.
- [14] a) J. Farkas, H. Peter, P. Christian, J. A. G. Urrea, M. Hassellöv, J. Tuoriniemi, S. Gustafsson, E. Olsson, K. Hylland, K. V. Thomas, *Environ. Int.* **2011**, *37*, 1057–1062; b) B. Nowack, J. F. Ranville, S. Diamond, J. A. Gallego-Urrea, C. Metcalfe, J. Rose, N. Horne, A. A. Koelmans, S. J. Klaine, *Environ. Toxicol. Chem.* **2012**, *31*, 50–59; c) A. Weir, P. Westerhoff, L. Fabricius, K. Hristovski, N. von Goetz, *Environ. Sci. Technol.* **2012**, *46*, 2242–2250.
- [15] A. A. Keller, S. McFerran, A. Lazareva, S. Suh, *J. Nanopart. Res.* **2013**, *15*, UNSP 1692.
- [16] F. Piccinno, F. Gottschalk, S. Seeger, B. Nowack, *J. Nanopart. Res.* **2012**, *14*, 1109.
- [17] C. O. Robichaud, A. E. Uyar, M. R. Darby, L. G. Zucker, M. R. Wiesner, *Environ. Sci. Technol.* **2009**, *43*, 4227–4233.
- [18] a) R. Kaegi, B. Sinnet, S. Zuleeg, H. Hagendorfer, E. Mueller, R. Vonbank, M. Boller, M. Burkhardt, *Environ. Pollut.* **2010**, *158*, 2900–2905; b) R. Kaegi, A. Ulrich, B. Sinnet, R. Vonbank, A. Wichser, S. Zuleeg, H. Simmler, S. Brunner, H. Vonmont, M. Burkhardt, M. Boller, *Environ. Pollut.* **2008**, *156*, 233–239.
- [19] a) D. Gohler, M. Stintz, L. Hillemann, M. Vorbau, *Ann. Occup. Hyg.* **2010**, *54*, 615–624; b) M. Vorbau, L. Hillemann, M. Stintz, *J. Aerosol Sci.* **2009**, *40*, 209–217.
- [20] T. M. Benn, P. Westerhoff, *Environ. Sci. Technol.* **2008**, *42*, 4133–4139.
- [21] a) M. E. Quadros, R. Pierson, N. S. Tulve, R. Willis, K. Rogers, T. A. Thomas, L. C. Marr, *Environ. Sci. Technol.* **2013**, *47*(15), 8894–8901; b) C. Lorenz, L. Windler, N. von Goetz, R. P. Lehmann, M. Schuppler, K. Hungerbühler, M. Heuberger, B. Nowack, *Chemosphere* **2012**, *89*, 817–824.
- [22] L. Geranio, M. Heuberger, B. Nowack, *Environ. Sci. Technol.* **2009**, *43*, 8113–8118.
- [23] Y. Echegoyen, C. Nerin, *Food Chem. Toxicol.* **2013**, *62*, 16–22.

- [24] N. von Goetz, L. Fabricius, R. Glaus, V. Weitbrecht, D. Gunther, K. Hungerbühler, *Food Addit. Contam. Part A* **2013**, *30*, 612–620.
- [25] B. Nowack, R. M. David, H. Fissan, H. Morris, J. A. Shatkin, M. Stintz, R. Zepp, D. Brouwer, *Environ. Int.* **2013**, *59*, 1–11.
- [26] C. Neal, H. Jarvie, P. Rowland, A. Lawler, D. Sleep, P. Scholefield, *Sci. Total Environ.* **2011**, *409*, 1843–1853.
- [27] N. O'Brien, E. Cummins, *Hum. Ecol. Risk Assess.* **2010**, *16*, 847–872.
- [28] E. Neubauer, F. D. von der Kammer, T. Hofmann, *Water Res.* **2013**, *47*, 2757–2769.
- [29] F. von der Kammer, S. Legros, E. H. Larsen, K. Loeschner, T. Hofmann, *TrAC-Trends Anal. Chem.* **2011**, *30*, 425–436.
- [30] A. P. Gondikas, F. von der Kammer, R. B. Reed, S. Wagner, J. F. Ranville, T. Hofmann, *Environ. Sci. Technol.* **2014**, *48*, 5415–5422.
- [31] T. Y. Sun, F. Gottschalk, K. Hungerbühler, B. Nowack, *Environ. Pollut.* **2014**, *185*, 69–76.
- [32] a) T. Yoshida, Y. Yoshioka, K. Matsuyama, Y. Nakazato, S. Tochigi, T. Hirai, S. Kondoh, K. Nagano, Y. Abe, H. Kamada, S. Tsunoda, H. Nabeshi, T. Yoshikawa, Y. Tsutsumi, *Biochem. Biophys. Res. Commun.* **2012**, *427*, 748–752; b) A. R. Whitley, C. Levard, E. Oostveen, P. M. Bertsch, C. J. Matocha, F. von der Kammer, J. M. Unrine, *Environ. Pollut.* **2013**, *182*, 141–149.
- [33] a) J. M. Zook, M. D. Halter, D. Cleveland, S. E. Long, *J. Nanopart. Res.* **2012**, *14*, 1165; b) M. Tejamaya, I. Römer, R. C. Merrifield, J. R. Lead, *Environ. Sci. Technol.* **2012**, *46*, 7011–7017; c) D. P. Stankus, S. E. Lohse, J. E. Hutchison, J. A. Nason, *Environ. Sci. Technol.* **2011**, *45*, 3238–3244.
- [34] T. L. Kirschling, P. L. Golas, J. M. Unrine, K. Matyjaszewski, K. B. Gregory, G. V. Lowry, R. D. Tilton, *Environ. Sci. Technol.* **2011**, *45*, 5253–5259.
- [35] M. Auffan, M. Pedetour, J. Rose, A. Masion, F. Ziarelli, D. Borschneck, C. Chaneac, C. Botta, P. Chaurand, J. Labille, J. Y. Bottero, *Environ. Sci. Technol.* **2010**, *44*, 2689–2694.
- [36] a) J. M. Pettibone, J. W. Hudgens, *Small* **2012**, *8*, 715–725; b) J. Liu, S. Legros, G. Ma, J. G. C. Veinot, F. von der Kammer, T. Hofmann, *Chemosphere* **2012**, *87*, 918–924; c) K. A. Huynh, K. L. Chen, *Environ. Sci. Technol.* **2011**, *45*, 5564–5571.
- [37] S. W. Bennett, D. X. Zhou, R. Mielke, A. A. Keller, *PLoS One* **2012**, *7*, e48719.
- [38] a) X. Zhang, M. Kah, M. T. O. Jonker, T. Hofmann, *Environ. Sci. Technol.* **2012**, *46*, 7166–7173; b) F. Sharif, P. Westerhoff, P. Herckes, *Environ. Sci. Proc. Impacts* **2013**, *15*, 267–274.
- [39] A. Mukhopadhyay, C. Grabinski, A. R. M. N. Afrooz, N. B. Saleh, S. Hussain, *Appl. Biochem. Biotechnol.* **2012**, *167*, 327–337.
- [40] J. M. Unrine, B. P. Colman, A. J. Bone, A. P. Gondikas, C. W. Matson, *Environ. Sci. Technol.* **2012**, *46*, 6915–6924.
- [41] a) J. Labille, J. Feng, C. Botta, D. Borschneck, M. Sammut, M. Cabie, M. Auffan, J. Rose, J. Y. Bottero, *Environ. Pollut.* **2010**, *158*, 3482–3489; b) S. Ottofuelling, F. Von Der Kammer, T. Hofmann, *Environ. Sci. Technol.* **2011**, *45*, 10045–10052.
- [42] a) J. T. K. Quik, I. Lynch, K. Van Hoecke, C. J. H. Miermans, K. A. C. De Schampelaere, C. R. Janssen, K. A. Dawson, M. A. C. Stuart, D. Van de Meent, *Chemosphere* **2010**, *81*, 711–715; b) W. Liu, J. Rose, S. Plantevin, M. Auffan, J. Y. Bottero, C. Vidaud, *Nanoscale* **2013**, *5*, 1658–1665.
- [43] R. Huang, R. P. Carney, F. Stellacci, B. L. T. Lau, *Nanoscale* **2013**, *5*, 6928–6935.
- [44] G. R. Aiken, H. Hsu-Kim, J. N. Ryan, *Environ. Sci. Technol.* **2011**, *45*, 3196–3201.
- [45] a) A. P. Gondikas, E. K. Jang, H. Hsu-Kim, *J. Colloid Interface Sci.* **2010**, *347*, 167–171; b) M. F. Hochella, Jr., S. K. Lower, P. A. Maurice, R. L. Penn, N. Sahai, D. L. Sparks, B. S. Twining, *Science* **2008**, *319*, 1631–1635; c) S. Kumpulainen, F. von der Kammer, T. Hofmann, *Water Res.* **2008**, *42*, 2051–2060; d) A. Deonarine, B. L. T. Lau, G. R. Aiken, J. N. Ryan, H. Hsu-Kim, *Environ. Sci. Technol.* **2011**, *45*, 3217–3223.
- [46] a) I. Heidmann, I. Christl, R. Kretzschmar, *Geochim. Cosmochim. Acta* **2005**, *69*, 1675–1686; b) A. F. Hofacker, A. Voegelin, R. Kaegi, F. A. Weber, R. Kretzschmar, *Geochim. Cosmochim. Acta* **2013**, *103*, 316–332; c) T. Hofmann, F. von der Kammer, *Environ. Pollut.* **2009**, *157*, 1117–1126; d) F. A. Weber, A. Voegelin, R. Kaegi, R. Kretzschmar, *Nat. Geosci.* **2009**, *2*, 267–271.
- [47] A. J. Bone, B. P. Colman, A. P. Gondikas, K. M. Newton, K. H. Harrold, R. M. Cory, J. M. Unrine, S. J. Klaine, C. W. Matson, R. T. Di Giulio, *Environ. Sci. Technol.* **2012**, *46*, 6925–6933.
- [48] L. Windler, C. Lorenz, N. von Goetz, K. Hungerbühler, M. Amberg, M. Heuberger, B. Nowack, *Environ. Sci. Technol.* **2012**, *46*, 8181–8188.
- [49] A. P. Gondikas, A. Morris, B. C. Reinsch, S. M. Marinakos, G. V. Lowry, H. Hsu-Kim, *Environ. Sci. Technol.* **2012**, *46*, 7037–7045.
- [50] a) A. S. Adeleye, A. A. Keller, R. J. Miller, H. S. Lenihan, *J. Nanopart. Res.* **2013**, *15*, 1418; b) B. C. Reinsch, B. Forsberg, R. L. Penn, C. S. Kim, G. V. Lowry, *Environ. Sci. Technol.* **2010**, *44*, 3455–3461.
- [51] a) B. Kim, M. Murayama, B. P. Colman, M. F. Hochella, Jr., *J. Environ. Monit.* **2012**, *14*, 1129–1137; b) V. Sternitzke, R. Kaegi, J. N. Audinot, E. Lewin, J. G. Hering, C. A. Johnson, *Environ. Sci. Technol.* **2012**, *46*, 802–809; c) K. Yin, I. M. C. Lo, H. Dong, P. Rao, M. S. H. Mak, *J. Hazard. Mater.* **2012**, 227–228, 118–125.
- [52] Z. Hu, G. Oskam, R. L. Penn, N. Pesika, P. C. Searson, *J. Phys. Chem. B* **2003**, *107*, 3124–3130.
- [53] N. D. Burrows, C. R. H. Hale, R. L. Penn, *Cryst. Growth Des.* **2012**, *12*, 4787–4797.
- [54] a) H. Zhang, J. R. Rustad, J. F. Banfield, *J. Phys. Chem. A* **2007**, *111*, 5008–5014; b) J. C. Myers, R. L. Penn, *J. Phys. Chem. C* **2007**, *111*, 10597–10602.
- [55] H. Zhang, B. Chen, Y. Ren, G. A. Waychunas, J. F. Banfield, *Phys. Rev. B* **2010**, *81*, 125444.
- [56] a) I. A. Mudunkotuwa, J. M. Pettibone, V. H. Grassian, *Environ. Sci. Technol.* **2012**, *46*, 7001–7010; b) J. Liu, D. A. Sonshine, S. Shervani, R. H. Hurt, *ACS Nano* **2010**, *4*, 6903–6913.
- [57] F. Larner, Y. Dogra, A. Dybowska, J. Fabrega, B. Stolpe, L. J. Bridgestock, R. Goodhead, D. J. Weiss, J. Moger, J. R. Lead, E. Valsami-Jones, C. R. Tyler, T. S. Galloway, M. Rehkamper, *Environ. Sci. Technol.* **2012**, *46*, 12137–12145.
- [58] a) R. L. Rebodos, P. J. Vikesland, *Langmuir* **2010**, *26*, 16745–16753; b) L. Charlet, G. Morin, J. Rose, Y. Wang, M. Auffan, A. Burnol, A. Fernandez-Martinez, *C. R. Geosci.* **2011**, *343*, 123–139; c) T. Echigo, D. M. Aruguete, M. Murayama, M. F. Hochella, *Geochim. Cosmochim. Acta* **2012**, *90*, 149–162.
- [59] R. L. Johnson, J. T. Nurmi, G. S. O. Johnson, D. Fan, R. L. O. Johnson, Z. Shi, A. J. Salter-Blanc, P. G. Tratnyek, G. V. Lowry, *Environ. Sci. Technol.* **2013**, *47*, 1573–1580.
- [60] B. P. Colman, C. L. Arnaout, S. Anciaux, C. K. Gunsch, M. F. Hochella, Jr., B. Kim, G. V. Lowry, B. M. McGill, B. C. Reinsch, C. J. Richardson, J. M. Unrine, J. P. Wright, L. Yin, E. S. Bernhardt, *PLoS One* **2013**, *8*, e57189.
- [61] C. L. Doolette, M. J. McLaughlin, J. K. Kirby, D. J. Batstone, H. H. Harris, H. Ge, G. Cornelis, *Chem. Cent. J.* **2013**, *7*, 46.
- [62] R. Kaegi, A. Voegelin, C. Ort, B. Sinnet, B. Thalmann, J. Krismer, H. Hagendorfer, M. Elumelu, E. Mueller, *Water Res.* **2013**, *47*, 3866–3877.
- [63] R. Kaegi, A. Voegelin, B. Sinnet, S. Zuleeg, H. Hagendorfer, M. Burkhardt, H. Siegrist, *Environ. Sci. Technol.* **2011**, *45*, 3902–3908.

- [64] G. V. Lowry, B. P. Espinasse, A. R. Badireddy, C. J. Richardson, B. C. Reinsch, L. D. Bryant, A. J. Bone, A. Deonarine, S. Chae, M. Therezien, B. P. Colman, H. Hsu-Kim, E. S. Bernhard, C. W. Matson, M. R. Wiesner, *Environ. Sci. Technol.* **2012**, *46*, 7027–7036.
- [65] B. Kim, C. S. Park, M. Murayama, M. F. Hochella, *Environ. Sci. Technol.* **2010**, *44*, 7509–7514.
- [66] J. Liu, K. G. Pennell, R. H. Hurt, *Environ. Sci. Technol.* **2011**, *45*, 7345–7353.
- [67] a) B. C. Reinsch, C. Levard, Z. Li, R. Ma, A. Wise, K. B. Gregory, G. E. Brown, G. V. Lowry, *Environ. Sci. Technol.* **2012**, *46*, 6992–7000; b) C. Levard, B. C. Reinsch, F. M. Michel, C. Oumahi, G. V. Lowry, G. E. Brown, *Environ. Sci. Technol.* **2011**, *45*, 5260–5266.
- [68] a) C. Levard, F. M. Michel, Y. Wang, Y. Choi, P. Eng, G. E. Brown, *J. Synchrotron Radiat.* **2011**, *18*, 871–878; b) C. Levard, E. M. Hotze, G. V. Lowry, G. E. Brown, *Environ. Sci. Technol.* **2012**, *46*, 6900–6914.
- [69] a) S. W. Bennett, A. Adeleye, Z. Ji, A. A. Keller, *Water Res.* **2013**, *47*, 4074–4085; b) S. R. Chae, A. R. Badireddy, J. F. Budarz, S. Lin, Y. Xiao, M. Therezien, M. R. Wiesner, *ACS Nano* **2010**, *4*, 5011–5018; c) S. R. Chae, E. M. Hotze, Y. Xiao, J. Rose, M. R. Wiesner, *Environ. Eng. Sci.* **2010**, *27*, 797–804; d) S. R. Chae, Y. Xiao, S. Lin, T. Noeiaghahi, J. O. Kim, M. R. Wiesner, *Water Res.* **2012**, *46*, 4053–4062; e) T. Hüffer, M. Kah, T. Hofmann, T. C. Schmidt, *Environ. Sci. Technol.* **2013**, *47*, 6935–6942.
- [70] S. R. Chae, Y. Watanabe, M. R. Wiesner, *Water Res.* **2011**, *45*, 308–314.
- [71] Y. Cheng, L. Yin, S. Lin, M. Wiesner, E. Bernhardt, J. Liu, *J. Phys. Chem. C* **2011**, *115*, 4425–4432.
- [72] a) S. Garg, A. L. Rose, T. D. Waite, *Geochim. Cosmochim. Acta* **2011**, *75*, 4310–4320; b) A. M. Jones, S. Garg, D. He, A. N. Pham, T. D. Waite, *Environ. Sci. Technol.* **2011**, *45*, 1428–1434.
- [73] C. Levard, S. Mitra, T. Yang, A. D. Jew, A. R. Badireddy, G. V. Lowry, G. E. Brown, *Environ. Sci. Technol.* **2013**, *47*, 5738–5745.
- [74] N. D. Burrows, V. M. Yuwono, R. L. Penn, *MRS Bull.* **2010**, *35*, 133–137.
- [75] D. J. Burleson, R. L. Penn, *Langmuir* **2006**, *22*, 402–409.
- [76] B. Gilbert, H. Zhang, F. Huang, M. P. Finnegan, G. A. Waychunas, J. F. Banfield, *Geochem. Trans.* **2003**, *4*, 20–27.
- [77] R. L. Penn, J. J. Erbs, D. M. Gulliver, *J. Cryst. Growth* **2006**, *293*, 1–4.
- [78] a) R. L. Penn, K. Tanaka, J. Erbs, *J. Cryst. Growth* **2007**, *309*, 97–102; b) H. Zhang, J. F. Banfield, *Chem. Mater.* **2005**, *17*, 3421–3425.
- [79] a) W. C. Hou, B. Stuart, R. Howes, R. G. Zepp, *Environ. Sci. Technol.* **2013**, *47*, 7713–7721; b) B. H. Gu, Y. R. Bian, C. L. Miller, W. M. Dong, X. Jiang, L. Y. Liang, *Proc. Natl. Acad. Sci. USA* **2011**, *108*, 1479–1483.
- [80] T. Zhang, B. Kim, C. Levard, B. C. Reinsch, G. V. Lowry, M. A. Deshusses, H. Hsu-Kim, *Environ. Sci. Technol.* **2012**, *46*, 6950–6958.
- [81] S. Kumpulainen, M. L. Räisänen, F. Von Der Kammer, T. Hofmann, *Clay Miner.* **2008**, *43*, 437–448.
- [82] S. A. Cumberland, J. R. Lead, *J. Chromatogr. A* **2009**, *1216*, 9099–9105.
- [83] R. Kretzschmar, D. Hesterberg, H. Sticher, *Soil Sci. Soc. Am. J.* **1997**, *61*, 101–108.
- [84] D. X. Zhou, A. A. Keller, *Water Res.* **2010**, *44*, 2948–2956.
- [85] R. Kretzschmar, H. Sticher, *Phys. Chem. Earth* **1998**, *23*, 133–139.
- [86] J. F. Mccarthy, J. M. Zachara, *Environ. Sci. Technol.* **1989**, *23*, 496–502.
- [87] R. Kretzschmar, W. P. Robarge, A. Amoozegar, *Environ. Sci. Technol.* **1994**, *28*, 1907–1915.
- [88] a) G. Cornelis, L. Pang, C. Doolette, J. K. Kirby, M. J. McLaughlin, *Sci. Total Environ.* **2013**, *463–464*, 120–130; b) M. Y. Chan, P. J. Vikesland, *Environ. Sci. Technol.* **2014**, *48*, 1532–1540.
- [89] A. R. Petosa, D. P. Jaisi, I. R. Quevedo, M. Elimelech, N. Tufenkji, *Environ. Sci. Technol.* **2010**, *44*, 6532–6549.
- [90] a) D. Zhou, A. I. Abdel-Fattah, A. A. Keller, *Environ. Sci. Technol.* **2012**, *46*, 7520–7526; b) A. R. M. N. Afrooz, I. A. Khan, S. M. Hussain, N. B. Saleh, *Environ. Sci. Technol.* **2013**, *47*, 1853–1860.
- [91] R. D. Handy, F. von der Kammer, J. R. Lead, M. Hasselov, R. Owen, M. Crane, *Ecotoxicology* **2008**, *17*, 287–314.
- [92] X. Y. Liu, G. X. Chen, A. A. Keller, C. M. Su, *Environ. Sci.-Proc. Imp* **2013**, *15*, 169–189.
- [93] O. Sagee, I. Dror, B. Berkowitz, *Chemosphere* **2012**, *88*, 670–675.
- [94] M. Baalousha, A. Manciualea, S. Cumberland, K. Kendall, J. R. Lead, *Environ. Toxicol. Chem.* **2008**, *27*, 1875–1882.
- [95] R. Arvidsson, S. Molander, B. A. Sandén, M. Hassellöv, *Hum. Ecol. Risk Assess.* **2011**, *17*, 245–262.
- [96] J. Ryu, W. Choi, *Environ. Sci. Technol.* **2008**, *42*, 294–300.
- [97] H. J. Kim, T. Phenrat, R. D. Tilton, G. V. Lowry, *J. Colloid Interface Sci.* **2012**, *370*, 1–10.
- [98] Y. H. Shih, W. S. Liu, Y. F. Su, *Environ. Toxicol. Chem.* **2012**, *31*, 1693–1698.
- [99] B. T. Lee, J. F. Ranville, *J. Hazard. Mater.* **2012**, *213–214*, 434–439.
- [100] R. F. Domingos, N. Tufenkji, K. J. Wilkinson, *Environ. Sci. Technol.* **2009**, *43*, 1282–1286.
- [101] J. Liu, S. Legros, F. Von Der Kammer, T. Hofmann, *Environ. Sci. Technol.* **2013**, *47*, 4113–4120.
- [102] M. Baalousha, Y. Nur, I. Römer, M. Tejamaya, J. R. Lead, *Sci. Total Environ.* **2013**, *454–455*, 119–131.
- [103] R. A. French, A. R. Jacobson, B. Kim, S. L. Isley, L. Penn, P. C. Baveye, *Environ. Sci. Technol.* **2009**, *43*, 1354–1359.
- [104] R. F. Domingos, C. Peyrot, K. J. Wilkinson, *Environ. Chem.* **2010**, *7*, 61–66.
- [105] N. B. Saleh, L. D. Pfefferle, M. Elimelech, *Environ. Sci. Technol.* **2010**, *44*, 2412–2418.
- [106] A. R. Petosa, S. J. Brennan, F. Rajput, N. Tufenkji, *Water Res.* **2012**, *46*, 1273–1285.
- [107] a) K. G. Li, W. Zhang, Y. Huang, Y. S. Chen, *J. Nanopart. Res.* **2011**, *13*, 6483–6491; b) X. Y. Liu, G. X. Chen, C. M. Su, *Environ. Sci. Technol.* **2012**, *46*, 6681–6688.
- [108] A. M. El Badawy, T. P. Luxton, R. G. Silva, K. G. Scheckel, M. T. Suidan, T. M. Tolaymat, *Environ. Sci. Technol.* **2010**, *44*, 1260–1266.
- [109] G. Chen, X. Liu, C. Su, *Environ. Sci. Technol.* **2012**, *46*, 7142–7150.
- [110] K. A. Huynh, J. M. McCaffery, K. L. Chen, *Environ. Sci. Technol.* **2012**, *46*, 5912–5920.
- [111] M. A. Kiser, H. Ryu, H. Y. Jang, K. Hristovski, P. Westerhoff, *Water Res.* **2010**, *44*, 4105–4114.
- [112] O. Furman, S. Usenko, B. L. T. Lau, *Environ. Sci. Technol.* **2013**, *47*, 1349–1356.
- [113] W. A. Shoults-Wilson, B. C. Reinsch, O. V. Tsyusko, P. M. Bertsch, G. V. Lowry, J. M. Unrine, *Nanotoxicology* **2011**, *5*, 432–444.
- [114] a) A. Hitchman, G. H. S. Smith, Y. Ju-Nam, M. Sterling, J. R. Lead, *Chemosphere* **2013**, *90*, 410–416; b) B. J. R. Thio, D. X. Zhou, A. A. Keller, *J. Hazard. Mater.* **2011**, *189*, 556–563.
- [115] S. Diegoli, A. L. Manciualea, S. Begum, I. P. Jones, J. R. Lead, J. A. Preece, *Sci. Total Environ.* **2008**, *402*, 51–61.
- [116] S. Lin, Y. Cheng, J. Liu, M. R. Wiesner, *Langmuir* **2012**, *28*, 4178–4186.
- [117] J. A. Nason, S. A. McDowell, T. W. Callahan, *J. Environ. Monit.* **2012**, *14*, 1885–1892.

- [118] T. Phenrat, J. E. Song, C. M. Cisneros, D. P. Schoenfelder, R. D. Tilton, G. V. Lowry, *Environ. Sci. Technol.* **2010**, *44*, 4531–4538.
- [119] J. Buffle, H. P. v. Leeuwen, *Environmental particles*, Lewis, Boca Raton, **1992**.
- [120] N. Tufenkji, M. Elimelech, *Environ. Sci. Technol.* **2004**, *38*, 529–536.
- [121] M. Baalousha, *Sci. Total Environ.* **2009**, *407*, 2093–2101.
- [122] T. Raychoudhury, N. Tufenkji, S. Ghoshal, *Water Res.* **2012**, *46*, 1735–1744.
- [123] J. F. Banfield, H. Zhang, *Nanoparticles in the Environment in Reviews in Mineralogy and Geochemistry, Vol. 44 No. 1*, Mineralogical Society of America, **2001**, pp. 1–58.
- [124] J. J. Erbs, T. S. Berquó, B. C. Reinsch, G. V. Lowry, S. K. Banerjee, R. L. Penn, *Geochim. Cosmochim. Acta* **2010**, *74*, 3382–3395.
- [125] J. Liu, D. M. Aruguete, J. R. Jinschek, J. D. Rimstidt, M. F. Hochella, Jr., *Geochim. Cosmochim. Acta* **2008**, *72*, 5984–5996.
- [126] W. Stumm, J. J. Morgan, *Aquatic chemistry: chemical equilibria and rates in natural waters, 3rd ed.*, Wiley, New York, **1996**.
- [127] J. Liu, R. H. Hurt, *Environ. Sci. Technol.* **2010**, *44*, 2169–2175.
- [128] R. B. Reed, D. A. Ladner, C. P. Higgins, P. Westerhoff, J. F. Ranville, *Environ. Toxicol. Chem.* **2012**, *31*, 93–99.
- [129] a) R. Ma, C. Levard, S. M. Marinakos, Y. Cheng, J. Liu, F. M. Michel, G. E. Brown, G. V. Lowry, *Environ. Sci. Technol.* **2012**, *46*, 752–759; b) J. Liu, D. M. Aruguete, M. Murayama, M. F. Hochella, Jr., *Environ. Sci. Technol.* **2009**, *43*, 8178–8183.
- [130] M. Auffan, J. Rose, J. Y. Bottero, G. V. Lowry, J. P. Jolivet, M. R. Wiesner, *Nat. Nanotechnol.* **2009**, *4*, 634–641.
- [131] J. Schmidt, W. Vogelsberger, *J. Solution Chem.* **2009**, *38*, 1267–1282.
- [132] R. D. Kent, P. J. Vikesland, *Environ. Sci. Technol.* **2012**, *46*, 6977–6984.
- [133] M. A. Maurer-Jones, M. P. S. Mousavi, L. D. Chen, P. Buhlmann, C. L. Haynes, *Chem. Sci.* **2013**, *4*, 2564–2572.
- [134] D. M. Cwiertny, G. J. Hunter, J. M. Pettibone, M. M. Scherer, V. H. Grassian, *J. Phys. Chem. C* **2009**, *113*, 2175–2186.
- [135] Z. W. Pan, J. Tao, Y. M. Zhu, J. F. Huang, M. P. Paranthaman, *Chem. Mater.* **2010**, *22*, 149–154.
- [136] R. Ma, C. Levard, F. M. Michel, G. E. Brown, G. V. Lowry, *Environ. Sci. Technol.* **2013**, *47*, 2527–2534.
- [137] a) K. M. Mullaugh, G. W. Luther, *J. Environ. Monit.* **2010**, *12*, 890–897; b) A. P. Gondikas, A. Masion, M. Auffan, B. L. T. Lau, H. Hsu-Kim, *Chem. Geol.* **2012**, *329*, 10–17.
- [138] J. Liu, Z. Wang, F. D. Liu, A. B. Kane, R. H. Hurt, *ACS Nano* **2012**, *6*, 9887–9899.
- [139] X. Y. Liu, V. Gurel, D. Morris, D. W. Murray, A. Zhitkovich, A. B. Kane, R. H. Hurt, *Adv. Mater.* **2007**, *19*, 2790–2796.